



Research article

Dynamical and optimal control analysis of a seasonal *Trypanosoma brucei rhodesiense* model

Mlyashimbi Helikumi^{1,2,*}, Moathodi Kgosimore³, Dmitry Kuznetsov¹ and Steady Mushayabasa^{4,*}

¹ Institution of Science and Technology (NM-AIST), School of Computational and Communication Science and Engineering, The Nelson Mandela African, P. O. Box 447, Arusha, Tanzania

² Department of Mathematics and Statistics, Mbeya University of Science and Technology, College of Science and Technical Education, P.O. Box 131, Mbeya, Tanzania

³ Department of Basic Sciences, Botswana University of Agriculture and Natural Resources Private Bag 0027, Gaborone, Botswana

⁴ Department of Mathematics, University of Zimbabwe, P.O. Box MP 167, Harare, Zimbabwe

* **Correspondence:** Email: helikumim@nm-aist.ac.tz, steadymushaya@gmail.com.

Abstract: The effects of seasonal variations on the epidemiology of *Trypanosoma brucei rhodesiense* disease is well documented. In particular, seasonal variations alter vector development rates and behaviour, thereby influencing the transmission dynamics of the disease. In this paper, a mathematical model for *Trypanosoma brucei rhodesiense* disease that incorporates seasonal effects is presented. Owing to the importance of understanding the effective ways of managing the spread of the disease, the impact of time dependent intervention strategies has been investigated. Two controls representing human awareness campaigns and insecticides use have been incorporated into the model. The main goal of introducing these controls is to minimize the number of infected host population at low implementation costs. Although insecticides usage is associated with adverse effects to the environment, in this study we have observed that by totally neglecting insecticide use, effective disease management may present a formidable challenge. However, if human awareness is combined with low insecticide usage then the disease can be effectively managed.

Keywords: *Trypanosoma brucei rhodesiense*; seasonality; stability; optimal control

1. Introduction

Vector-borne diseases, such as dengue virus, Zika virus, malaria, yellow fever and human African trypanosomiasis (HAT) are known to be highly sensitive to environmental changes, including

variations in climate and land-surface characteristics [1]. Seasonal variations in climatic factors, such as rainfall and temperature have a strong influence on the life cycle of vector thereby affecting the distribution and abundance of vectors seasonally [2]. For example, tsetse flies-vectors responsible for transmission of trypanosomiasis infection in humans and animals need a particular temperature (16–38 °C) and humidity (50–80% of relative humidity) to survive [3]. Therefore, they are linked to the presence of water that increases the local humidity, allowing for the growth of vegetation that protects them from direct sunlight and wind, and attracts the animals to where tsetse feed [3–5]. Therefore, as suggested by Leak [6] understanding the relationship between these factors and vector population dynamics is therefore a potential area for modelling and further development of existing models.

The main goal of this study is to understand the effects of seasonal variations on the transmission and control of *Trypanosoma brucei rhodesiense*. An analysis of *Trypanosoma brucei rhodesiense* datasets for Uganda demonstrated that the disease has seasonal variations with incidence higher during January, February, and March [7]. Another analysis of *Trypanosoma brucei rhodesiense* datasets for Maasai Steppe ecosystem of Tanzania also revealed marked seasonal variations on disease incidence [2, 8, 9]. *Trypanosoma brucei rhodesiense* is one of the two forms of Human African trypanosomiasis (HAT) a neglected disease that affects approximately 70 million people living in 1.55 million km² of sub-Saharan Africa [10, 11]. *Trypanosoma brucei rhodesiense* is prevalent in Eastern and Southern Africa while the other form *Trypanosoma brucei gambiense* is common in West and Central Africa [3]. According the World Health Organization (WHO), in 2015, 2804 cases of HAT were recorded, with 2733 attributed to *Trypanosoma brucei gambiense* (90% reduction since 1999) and 71 were attributed to *Trypanosoma brucei rhodesiense* (89% reduction since 1999); this number includes cases diagnosed in both endemic and non-endemic countries [12].

Despite an ambitious campaign led by WHO, many non-governmental organizations, and a public-private which managed to reduce HAT cases to less than 3000 in 2015 leading to the plans to eliminate HAT as a public health problem by 2020 [10], the disease is still endemic in some parts of sub-Saharan Africa, where it is a considerable burden on rural communities [12]. It is therefore essential to gain a better and more comprehensive understanding of effective ways to control disease in human and animal populations. In this study, we will evaluate the effects of optimal human awareness and insecticides use on controlling the spread of *Trypanosoma brucei rhodesiense* in a periodic environment. Effective management and control of *Trypanosoma brucei rhodesiense* has been regarded as complex, since disease transmission involves domestic animals, which serve as reservoirs for parasite transmission by the tsetse vector [10].

Mathematical models have proved to be an effective tool to investigate the long term dynamics of several infectious diseases. Several mathematical models have been proposed to qualitatively and quantitatively analyze the transmission and control of HAT [13–28]. Ackley et al. [16] developed a dynamic model with the goal to estimate tsetse fly mortality from ovarian dissection data in populations where age distribution is not essentially stable. One of the important results from their study was that mortality increases with temperature and this result is concurs with existing field and laboratory findings. Lord and co-workers [17] utilised a mathematical model to explore the effects of temperature on mortality, larviposition and emergence rates in tsetse vectors. Results from the work of Lord et al. [17] suggested that an increase in temperature maybe associated with the decline on tsetse abundance in Zimbabwe's Zambezi Valley. They also hypothesised that rising temperatures

may have made some higher, cooler, parts of Zimbabwe more suitable for tsetse leading to the emergence of new disease foci. Alderton et al. [18] proposed an agent-based model to assess the impact of seasonal climatic drivers on trypanosomiasis transmission rates. Simulation results from the work of Alderton et al. [18] demonstrated a perfect fit with observed HAT datasets thereby demonstrating that seasonality is key component on trypanosomiasis transmission rates. Stone and Chitnis [19] employed a system of ordinary differential equations (ODEs) to model to assess the implications of heterogeneous biting exposure and animal hosts on *Trypanosomiasis brucei gambiense* transmission and control. The work of Stone and Chitnis [19] had several outcomes, but overall, their study demonstrated that effective control of HAT hinges on understanding the ecological and environmental context of the disease, particularly for moderate and low transmission intensity settings.

Despite these efforts, none of the aforementioned works assessed the effects of optimal human awareness and insecticides use on long-term dynamics *Trypanosoma brucei rhodesiense* in a periodic environment. Thus in this study we will develop a periodic model for *Trypanosoma brucei rhodesiense* with an aim to evaluate the effects of optimal human awareness and insecticides use on long-term dynamics of the disease. As in [13, 19, 21, 22, 28], the proposed model assumes that both humans and animals are hosts for *Trypanosoma brucei rhodesiense*. Epidemiological stages of the disease that are sensitivity to seasonal variations have been modeled by periodic functions, such stages includes vector recruitment rate, natural mortality of vectors, vector biting rate and vector incubation period. Mathematical analysis and optimal control are applied to study the dynamical behavior of the model with and without optimal strategies. Overall, the results from the study demonstrated the strength of optimal control strategies on shaping long term dynamics of the disease. In particular, we have noted that effective control of the disease can be attained if optimal human awareness is coupled with insecticides use (even at extremely low intensity than when it is absent).

This paper is organized as follows. In section 2, we present the methods and results. In particular, we present periodic model for *Trypanosoma brucei rhodesiense*. The basic reproduction number of the model is computed and qualitatively used to show that it is an important threshold quantity that determines disease eradication or persistence in the community. We also extend the model to incorporate optimal human awareness and insecticide use. The main aim of introducing controls is to minimize the numbers of humans that are infected with disease over time at minimal costs. With the aid of optimal control theory, necessary conditions to achieve effective disease management in the presents of controls has been established. Finally, a brief discussion rounds up the paper in section 3.

2. Methods and results

2.1. Model formulation and boundedness of solutions

We consider a periodic ordinary differential equations model that incorporates the interplay between the vectors (tsetse flies) and two hosts (humans and animals). The compartments used for each population represents the epidemiological status of the species. Throughout this study, we will use the subscript a , h and v to denote variables or parameter associated with animals, humans and vector, respectively. Thus, each host population is subdivided into compartments of: Susceptible $S_i(t)$, exposed $E_i(t)$, infectious $I_i(t)$ and temporary immune $R_i(t)$, for $i = a, h$. Furthermore, the vector population is subdivided into compartments of: Susceptible $S_v(t)$, exposed $E_v(t)$ and infectious $I_v(t)$.

Thus, the total population of the hosts and vector at time t , denoted by $N_i(t)$ ($i = a, h$) and $N_v(t)$, respectively is given by

$$N_i(t) = S_i(t) + E_i(t) + I_i(t) + R_i(t), \quad N_v(t) = S_v(t) + E_v(t) + I_v(t).$$

The susceptible hosts (animals or humans) can acquire infection when they are bitten by an infectious tsetse vector. In this model, the following forces of infection describe vector-to-host disease transmission:

$$\lambda_h(t) = \frac{\sigma_v(t)N_v(t)\sigma_h}{\sigma_v(t)N_v(t) + \sigma_h N_h(t)} \beta_{vh} \frac{I_v(t)}{N_v(t)}, \quad \text{and,} \quad \lambda_a(t) = \frac{\sigma_v(t)N_v(t)\sigma_a}{\sigma_v(t)N_v(t) + \sigma_a N_a(t)} \beta_{va} \frac{I_v(t)}{N_v(t)}. \quad (1)$$

The parameter β_{vi} is the probability of infection from an infectious vector to a susceptible host i given that a contact between the two occurs, σ_a and σ_h represents the maximum number of vector bites an animal host and human host can sustain per unit time, respectively. The parameter,

$$\sigma_v(t) = \sigma_{v0} \left\{ 1 - \sigma_{v1} \cos \left(\frac{2\pi}{365} (t + \tau) \right) \right\},$$

represents the frequency of feeding activity by the tsetse flies and is also known as the vector biting rate, σ_{v0} is the average vector biting rate, and σ_{v1} defines the amplitude of seasonal variations (degree of periodic forcing, $0 < \sigma_{v1} < 1$), τ is a phase-shifting parameter to capture the timing of seasonality. Also note that a one year cycle has been considered, that is, $\omega = \frac{2\pi}{365}$. Prior studies suggests that vector biting depends on seasonal variations. Precisely, the vector development rates and behaviour, depends on seasonal variations [13, 29]. Furthermore, $\sigma_v(t)N_v(t)$ denotes the total number of bites that the tsetse vectors would like to achieve in unit time, $\sigma_a N_a(t)$ and $\sigma_h N_h(t)$ denotes the availability of hosts. The total number of tsetse-host contacts is half the harmonic mean of $\sigma_v(t)N_v(t)$ and $\sigma_i N_i(t)$ for $i = a, h$.

In addition, once infected, the susceptible host progresses to the exposed state, where they incubate the disease for $1/\kappa_i$ days, ($i = a, h$) before they progress to the infectious stage. Infectious hosts recover from infection with temporary immunity through treatment at rate α_i , ($i = a, h$), which is inversely proportional to the average duration of the infectious period. Infectious hosts that fail to recover from infection succumb to disease-related death at rate d_i . It is assumed that temporary immunity wanes out at rate γ_i ($i = a, h$) and they become susceptible to infection again. Birth and natural mortality rates of the hosts are modelled by b_i and μ_i , ($i = a, h$), respectively. We assume that there is no vertical transmission of the disease, hence all new recruits are assumed to be susceptible.

In this study, susceptible vectors are assumed to acquire infection when they bite an infectious host and the following force of infection accounts for disease transmission in this case:

$$\lambda_v(t) = \frac{\sigma_v(t)\sigma_h N_h(t)}{\sigma_v(t)N_v(t) + \sigma_h N_h(t)} \beta_{hv} \frac{I_h(t)}{N_h(t)} + \frac{\sigma_v(t)\sigma_a N_a(t)}{\sigma_v(t)N_v(t) + \sigma_a N_a(t)} \beta_{va} \frac{I_a(t)}{N_a(t)}. \quad (2)$$

The parameter β_{hv} represents the probability of infection from an infectious human to a susceptible vector given that a contact between the two occurs, β_{av} is the probability that disease transmission occurs whenever there is sufficient contact between a susceptible vector and an infectious animal. In the absence of seasonal forcing, the forces of infection considered in this study, that is, Eqs (1) and (2), are isomorphic to the ones proposed in [30, 31]. Upon infection, the vector moves to the exposed class and they progress to the infectious stage at rate

$$\kappa_v(t) = \kappa_{v0} [1 - \kappa_{v1} \cos(\omega t + \tau)],$$

κ_{v_0} denotes the average incubation rate in the absence of seasonal variations and κ_{v_1} ($0 < \kappa_{v_1} < 1$) is the amplitude of the seasonal variation. In addition, vector recruitment rate $b_v(t)$ and natural mortality rate $\mu_v(t)$ have been assumed to follow seasonal variations with

$$b_v(t) = b_{v_0}[1 - b_{v_1} \cos(\omega t + \tau)], \quad \text{and} \quad \mu_v(t) = \mu_{v_0}[1 - \mu_{v_1} \cos(\omega t + \tau)],$$

where b_{v_0}, μ_{v_0} denotes the average birth and natural mortality rates, respectively, and b_{v_1} ($0 < b_{v_1} < 1$) μ_{v_1} ($0 < \mu_{v_1} < 1$) is the amplitude of the seasonal variation. Infectious vectors are assumed to remain in that state for their entire lifespan.

Based on assumptions above, with all model variables and parameters assumed to be non-negative, the following system of nonlinear ordinary differential equations summaries the dynamics of *Trypanosoma brucei rhodesiense* disease:

$$\left. \begin{aligned} S'_h(t) &= b_h N_h(t) - \lambda_h(t) S_h(t) - \mu_h S_h(t) + \gamma_h R_h(t), \\ E'_h(t) &= \lambda_h(t) S_h(t) - (\mu_h + \kappa_h) E_h(t), \\ I'_h(t) &= \kappa_h E_h(t) - (\mu_h + \alpha_h + d_h) I_h(t), \\ R'_h(t) &= \alpha_h I_h(t) - (\mu_h + \gamma_h) R_h(t), \\ S'_a(t) &= b_a N_a(t) - \lambda_a(t) S_a(t) - \mu_a S_a(t) + \gamma_a R_a(t), \\ E'_a(t) &= \lambda_a(t) S_a(t) - (\mu_a + \kappa_a) E_a(t), \\ I'_a(t) &= \kappa_a E_a(t) - (\mu_a + \alpha_a + d_a) I_a(t), \\ R'_a(t) &= \alpha_a I_a(t) - (\mu_a + \gamma_a) R_a(t), \\ S'_v(t) &= b_v(t) N_v(t) - \lambda_v(t) S_v(t) - \mu_v(t) S_v(t), \\ E'_v(t) &= \lambda_v(t) S_v(t) - (\kappa_v(t) + \mu_v(t)) E_v(t), \\ I'_v(t) &= \kappa_v(t) E_v(t) - \mu_v(t) I_v(t), \end{aligned} \right\} \quad (3)$$

subject to the initial values:

$$\left\{ \begin{array}{llll} S_h(0) = S_{h0} \geq 0, & E_h(0) = E_{h0} \geq 0, & I_h(0) = I_{h0} \geq 0, & R_h(0) = R_{h0} \geq 0, \\ S_a(0) = S_{a0} \geq 0, & E_a(0) = E_{a0} \geq 0, & I_a(0) = I_{a0} \geq 0, & R_a(0) = R_{a0} \geq 0, \\ S_v(0) = S_{v0} \geq 0, & E_v(0) = E_{v0} \geq 0, & I_v(0) = I_{v0} \geq 0. & \end{array} \right.$$

From the detailed computations in Appendix A, we conclude that the solutions $(S_h(t), E_h(t), I_h(t), R_h(t), S_a(t), E_a(t), I_a(t), R_a(t), S_v(t), E_v(t), I_v(t))$ of the model (3) are uniformly and ultimately bounded in

$$\Omega = \left\{ \left(\begin{array}{l} S_h(t) + E_h(t) + I_h(t) + R_h(t) \\ S_a(t) + E_a(t) + I_a(t) + R_a(t) \\ S_v(t) + E_v(t) + I_v(t) \end{array} \right) \in \mathbb{R}_+^{11} \left| \begin{array}{l} N_h(t) \leq N_{h0}, \\ N_a(t) \leq N_{a0}, \\ N_v(t) \leq N_{v0} \end{array} \right. \right\},$$

with $N_h(0) = N_{h0}$, $N_a(0) = N_{a0}$ and $N_v(0) = N_{v0}$. Therefore we can conclude that model (3) is epidemiologically and mathematically well-posed in the region Ω for all $t \geq 0$.

2.2. Extinction and uniform persistence of the disease

In order to determine the extinction and uniform persistence of the disease we will begin by computing the reproduction number of system (3). Often denoted by \mathcal{R}_0 , the reproduction number is an epidemiologically important threshold value which determines the ability of an infectious disease

invading a population. It can be determined by utilizing the next-generation matrix method [32]. Based on the computations in Appendix B, the basic reproduction number of the time-averaged autonomous system is

$$[\mathcal{R}_0] = \sqrt{\mathcal{R}_{0h} + \mathcal{R}_{0a}},$$

where

$$\begin{aligned} \mathcal{R}_{0h} &= \left(\frac{\kappa_h \beta_{vh} N_{h0} \kappa_{v0} \beta_{hv} N_{v0}}{\mu_{v0} (\kappa_{v0} + \mu_{v0}) (\kappa_h + \mu_h) (\mu_h + \alpha_h + d_h)} \right) \left(\frac{\sigma_h \sigma_{v0}}{\sigma_{v0} N_{v0} + \sigma_h N_{h0}} \right)^2, \\ \mathcal{R}_{0a} &= \left(\frac{\kappa_a \beta_{va} N_{a0} \kappa_{v0} \beta_{av} N_{v0}}{\mu_{v0} (\kappa_{v0} + \mu_{v0}) (\kappa_a + \mu_a) (\mu_a + \alpha_a + d_a)} \right) \left(\frac{\sigma_a \sigma_{v0}}{\sigma_{v0} N_{v0} + \sigma_a N_{a0}} \right)^2. \end{aligned}$$

The threshold quantities \mathcal{R}_{0h} and \mathcal{R}_{0a} represents the power of the disease to invade the human and animal host, respectively. Due to several time-dependent parameters in model (3), a detailed derivation of the seasonal reproduction number is presented in Appendix B. Furthermore, in Appendix B, we have also demonstrated that the reproduction number \mathcal{R}_0 is an important threshold parameter for disease extinction and persistence. In particular, the results show that when $\mathcal{R}_0 < 1$, model (3) admits a globally asymptotically stable disease-free equilibrium and if $\mathcal{R}_0 > 1$, the disease persists.

2.3. The optimal control problem

2.3.1. Model formulation

There are no vaccines for HAT but there exists a couple of preventative and treatment options. The main goal of the preventative strategies is to reduce contact between the hosts and vectors. Preventative strategies include use of trypanocides or insecticides. In addition, humans can also minimize vector contact by clothing on long-sleeved garments of medium-weight material with neutral colors that blend with the background environment. Prior studies have shown that insecticides or trypanocides use can be an effect strategy to control HAT [15]. However, it is worth noting that insecticides are expensive and individuals in many HAT endemic areas are may not be able to afford the cost. Moreover, excessive use of insecticides is associated with environmental adverse effects. Hence, there is need to investigate the effects of coupling insecticides use and other disease control mechanisms on long-term disease dynamics. In particular, a coupling in which low intensity use of insecticides would be more preferable. Thus, in this section, we seek to evaluate the impact of optimal and cost-effective media campaigns and insecticides use on long-term *Trypanosoma brucei rhodesiense* dynamics in a periodic environment. Once humans are aware of the disease they have the potential to minimize contact between the vectors and multiple species. In order to make this assessment, we extend model (3) to incorporate two controls $u_1(t)$ and $u_2(t)$, that represents time dependent media campaigns and insecticides use. These control will be assigned reasonable lower and upper bounds to reflect their limitations. Utilizing the same variables and parameter names as before (model (3)), the extended model with controls takes the form:

$$\left. \begin{aligned}
 S'_h(t) &= b_h N_h(t) - \lambda_h(t) S_h(t) - \mu_h S_h(t) - u_1(t) S_h(t) + \gamma_h R_h(t), \\
 E'_h(t) &= \lambda_h(t) S_h(t) - (\mu_h + \kappa_h) E_h(t), \\
 I'_h(t) &= \kappa_h E_h(t) - (\mu_h + \alpha_h + d_h) I_h(t), \\
 R'_h(t) &= u_1(t) S_h(t) + \alpha_h I_h(t) - (\mu_h + \gamma_h) R_h(t), \\
 S'_a(t) &= b_a N_a(t) - \lambda_a(t) S_a(t) - \mu_a S_a(t) + \gamma_a R_a(t), \\
 E'_a(t) &= \lambda_a(t) S_a(t) - (\mu_a + \kappa_a) E_a(t), \\
 I'_a(t) &= \kappa_a E_a(t) - (\mu_a + \alpha_a + d_a) I_a(t), \\
 R'_a(t) &= \alpha_a I_a(t) - (\mu_a + \gamma_a) R_a(t), \\
 S'_v(t) &= b_v(t) N_v(t) - \lambda_v(t) S_v(t) - (\mu_v(t) + u_2(t)) S_v(t), \\
 E'_v(t) &= \lambda_v(t) S_v(t) - (\kappa_v(t) + \mu_v(t) + u_2(t)) E_v(t), \\
 I'_v(t) &= \kappa_v(t) E_v(t) - (\mu_v(t) + u_2(t)) I_v(t),
 \end{aligned} \right\} \quad (4)$$

subject to the initial values:

$$\left\{ \begin{aligned}
 S_h(0) &= S_{h0} \geq 0, & E_h(0) &= E_{h0} \geq 0, & I_h(0) &= I_{h0} \geq 0, & R_h(0) &= R_{h0} \geq 0, \\
 S_a(0) &= S_{a0} \geq 0, & E_a(0) &= E_{a0} \geq 0, & I_a(0) &= I_{a0} \geq 0, & R_a(0) &= R_{a0} \geq 0, \\
 S_v(0) &= S_{v0} \geq 0, & E_v(0) &= E_{v0} \geq 0, & I_v(0) &= I_{v0} \geq 0.
 \end{aligned} \right.$$

Observe that in system (4), it is assumed that humans who become aware of the disease have negligible chances of acquiring the infection, and also insecticide use affects all the epidemiological classes of the vector populations. Further more, we assume that $u_i(t)$ ranges between 0 and q_i , that is $0 \leq u_i(t) \leq q_i < 1$, such that $u_i = 0$ reflects the absence of time dependent controls and q_i represents the upper bound of the control. The control set is

$$U = \left\{ (u_1, u_2) \in (L^\infty(0, t_f)) : 0 \leq u_i \leq q_i < 1, \quad q_i \in \mathbb{R}^+, \quad i = 1, 2. \right\}.$$

In developing response plans for effective management of diseases, policy makers seek optimal responses that can minimize the incidence and/or disease-related mortality rate while considering the cost of each mitigation strategy. Here, our goal is to minimize the number of infectious host (humans and animals) at minimal costs associated with strategy implementation. Thus the objective functional is given by

$$J(u_1(t), u_2(t)) = \int_0^{t_f} \left(C_1 I_h(t) + C_2 I_a(t) + \frac{W_1}{2} u_1^2(t) + \frac{W_2}{2} u_2^2(t) \right) dt, \quad (5)$$

subject to the constraints of the ODEs in system (4) and where C_1 , C_2 , W_1 and W_2 are positive constants also known as the balancing coefficients and their goal is to transfer the integral into monetary quantity over a finite time interval $[0, t_f]$. In (5) control efforts are assumed to be nonlinear-quadratic, since a quadratic structure in the control has mathematical advantages such as: If the control set is a compact and convex it follows that the Hamiltonian attains its minimum over the control set at a unique point. The basic framework of an optimal control problem is to prove the existence of an optimal control and then characterize it. Pontryagin's Maximum Principle is used to establish necessary conditions that must be satisfied by an optimal control solution [33]. Derivations on the existence of an optimal control pair as well as the necessary conditions that must be satisfied by optimal control solutions of system (4) are shown in Appendix C.

2.3.2. Numerical results and discussion

In this section, we present some numerical results of the proposed optimal control problem, (system(4)). The numerical solutions were obtained after solving the optimality system of eleven ordinary differential equations from the state and costate equations. The technique used is commonly known as the forward-backward sweep iterative method [34]. The first step of the forward-backward sweep method entails solving of the state equations with a guess for the controls over the simulated time using fourth-order Runge-Kutta scheme. “The controls are then updated by using a convex combination of the previous controls and the value from the characterizations of the controls. This process is repeated and iterations are ceased if the values of the unknowns at the previous iterations are very close to the ones at the present iterations” [34]. Table 1, below presents the essential steps carried out, for a detailed discussion we refer the reader to [34].

Table 1. Forward-backward sweep iterative method.

Algorithm
1. Subdivide the time interval $[t_0, t_f]$ into N equal subintervals. Set the state variable at different times as $x = x(t)$ and assume a piecewise-constant control $u_j^{(0)}(t)$, $t \in [t_k, t_{k+1}]$, where $k = 0, 1, 2, \dots, N - 1$ and $j = 1, 2$.
2. Apply the assumed control $u_j^{(0)}(t)$ to integrate the state system with an initial condition $x(t_0) = \mathbf{x}(0)$, forward in time $[t_0, t_f]$ using the fourth-order Runge-Kutta method, where $\mathbf{x}_0 = (S_h(0), E_h(0), I_h(0), R_h(0), S_a(0), E_a(0), I_a(0), R_a(0), S_v(0), E_v(0), I_v(0))$.
3. Apply the assumed control $u_j^{(0)}(t)$ to integrate the costate system with the transversality condition $\vec{\lambda}(t_f) = \lambda_i(t_f)$, $i = 1, 2, 3, \dots, 11$, backward in time $[t_0, t_f]$ using the fourth-order Runge-Kutta method.
4. Update the control by entering the new state and costate solutions $\vec{x}(t)$ and $\vec{\lambda}(t_f)$, respectively, through the characterization Eq (16) (see, Appendix C).
5. STOP the algorithm if $\frac{\ \vec{x}^{\vec{x}+1} - \vec{x}^{\vec{x}}\ }{\ \vec{x}^{\vec{x}+1}\ } < \xi$; otherwise update the control using a convex combination of the current and previous control and GO to step 2. Here, $\vec{x}^{\vec{x}}$ is the i^{th} iterative solution of the state system and ξ is an arbitrarily small positive quantity (Tolerance level).

On simulating system (4) we assumed the following initial population levels: $S_h = 10000$, $E_h = 0$, $I_h = 500$, $R_h = 0$, $S_a = 5000$, $E_a = 0$, $I_a = 350$, $R_a = 0$, $S_v = 20000$, $E_v = 0$, $I_v = 1000$. Furthermore, the weight constants W_1 and W_2 are varied. In the simulations we assume that $C_2 = 2C_1$ (with C_1 fixed to unity), that is, minimization of the infected humans has more importance/weight compare to that of infected animals. Furthermore, the rest of the parameter values used were taken from Table 2, majority of parameters values were adopted from the work of Moore et al. [13] as well as Ndondo et al. [22], while a few were assumed within realistic ranges due to their unavailability.

The total number of new infections in human and cattle population were determined by the following formulas, respectively

$$T_h = \int^{t_f} \left(\frac{\sigma_v(t)N_v\sigma_h}{\sigma_v(t)N_v + \sigma_h N_h} \beta_{vh} \frac{I_v}{N_v} S_h \right) dt,$$

$$T_a = \int^{t_f} \left(\frac{\sigma_v(t)N_v\sigma_a}{\sigma_v(t)N_v + \sigma_a N_a} \beta_{va} \frac{I_v}{N_v} S_a \right) dt.$$

and the total cost associated with infected animals, infected humans and the controls J , which is given by (5).

Table 2. Description of model parameters of system (3), indicating baseline, ranges and references.

Symbol	Description			
b_a, b_h	Birth rate for the hosts	$\frac{1}{15 \times 365}, \frac{1}{50 \times 365}$	Day ⁻¹	[22]
b_{v0}	Averaged birth rate of the vectors	$\frac{1}{33}$	Day ⁻¹	[22]
μ_{v0}	Averaged mortality rate of the vectors	$\frac{1}{33}$	Day ⁻¹	[22]
μ_a, μ_h	Natural mortality rate for the hosts	$\frac{1}{15 \times 365}, \frac{1}{50 \times 365}$	Day ⁻¹	[22]
d_a, d_h	Disease-induced death rate for the hosts	0.0008, $\frac{1}{108}$	Day ⁻¹	[13]
κ_{v0}	Average incubation rate for the vectors	$\frac{1}{25}(\frac{1}{25} - \frac{1}{30})$	Day ⁻¹	[22]
κ_a, κ_h	Incubation rate for the hosts	$\frac{1}{12}(\frac{1}{10} - \frac{1}{14})$	Day ⁻¹	[22]
σ_{v0}	Average vector biting rate	$\frac{1}{4}(\frac{1}{10} - \frac{1}{3})$	Day ⁻¹	[22]
σ_{v1}	Amplitude of oscillations in $\sigma_v(t)$, respectively	0.8	Dimensionless	
b_{v1}	Amplitude of oscillations in $b_v(t)$, respectively	0.8	Dimensionless	
μ_{v1}	Amplitude of oscillations in $\mu_v(t)$, respectively	0.8	Dimensionless	
κ_{v1}	Amplitude of oscillations in $\kappa_v(t)$, respectively	0.8	Dimensionless	
τ	Phase-shifting parameter	50	Days	
σ_a, σ_h	The maximum number of vector bites the host can have per unit time. This is a function of the host's exposed surface area and any vector control interventions used by the host to reduce exposure to tsetse vectors.	0.62, 0.7	Day ⁻¹	[22]
α_a, α_h	Recovery rate of the infectious host	$\frac{1}{25}, \frac{1}{30}$	Day ⁻¹	[22]
γ_a, γ_h	Immunity waning rate for the recovered host	$\frac{1}{75}, \frac{1}{90}$	Day ⁻¹	[22]
β_{va}, β_{vh}	Probability of infection from an infectious vector to a susceptible host given that a contact between the two occurs	0.62		[22]
β_{av}, β_{hv}	Probability that a vector becomes infected after biting an infectious animal, human	0.01		[22]

Simulation results in Figure 1 illustrates *Trypanosoma brucei rhodesiense* dynamics in the host and vector population, in the presence human awareness only, that is $0 \leq u_1(t) \leq 0.003$ and $u_2(t) = 0$. Overall, we can note that in the presence of optimal human awareness, the numbers of infected hosts and vectors is low compared to without optimal control. Furthermore, with optimal control, the numbers of infected host and vector converges to the disease-free equilibrium in a short time than when there is no optimal control. In addition, we noted that, the total number of infected human and

animal without control over a 2000 day period is $T_h = 4,535$ and $T_a = 2,471$, respectively, while in the presence of optimal human awareness campaigns only, the total number of infected human and animal population for the same period is $T_h = 2,985$ and $T_a = 1,9039$, respectively and the associated total costs of implementing the strategy is $J = 14,994$. Based on these results, one can conclude that the presence of optimal human awareness leads to reduction on cumulative infections for the human and animal host by $T_h = 1,550$ and $T_a = 567$, respectively. Comparing the infection reduction relative to the total number of infections recorded in without optimal control, it follows that, there is a 34.2% and 22.9% reduction in human and animal population, respectively. Figure 2 illustrates the control profile of $u_1(t)$, (note that $u_2(t) = 0$). We can see that, the control profile starts at its maxima and remains there for the entire time horizon. It gradually drops to its minima at the final horizon. This signifies that to attain the above results control $u_1(t)$ may need to be maintained at its maximum intensity for almost the entire time horizon.

Numerical results in Figure 3, illustrates the effects of combining optimal human awareness and insecticides use on long term *Trypanosoma brucei rhodesiense* dynamics in a periodic environment over 2000 days (we set $0 \leq u_1(t) \leq 0.003$ and $0 \leq u_2(t) \leq 0.001$, with $W_1 = 0.1$ and $W_2 = 100$). Once again we can observe that with optimal control strategies in place, few infections will be recorded compared to when there are no optimal control strategies. Precisely, with optimal control strategies in place, the total number of new infections over 2000 days is $T_h = 2,368$ and $T_a = 1,741$, for human and animal populations, respectively, and the associated costs of implementation is $J = 19,264$. We have also noted that without optimal control strategies, the total number of new infections for the human and animal host over 2000 days is 5,336 and 2,703 respectively. It follows that the optimal control strategies associated would have averted 2,368 and 962 infections in human and animal populations. This represents approximately 44% and 36% reduction of infections in human and animal populations, in relation to when there are no controls. Comparing the results in Figures 1 and 3, we can note that combining optimal human awareness and insecticides use, leads to effective disease management in a short period (convergence of solutions to the disease-free equilibrium in Figure 3 takes less time than in Figure 1) compared to when there is optimal human awareness alone.

Simulation results in Figure 4 depicts the control profiles for $u_1(t)$ and $u_2(t)$ over 2000 days. We can observe that all the control profiles starts at their respective maximums and remain there for the greater part of the time horizon, in particular, the control profile for $u_1(t)$ drops on the final time while that of $u_2(t)$ drops just before the final time. These results suggests that for this scenario both controls can be maintained at their respective maximum intensities in order to effectively manage the spread of the disease.

In Figure 5, we varied the bounds of the controls; human awareness $u_1(t)$ and insecticides use $u_2(t)$. We set we set $0 \leq u_1(t) \leq 0.03$ and $0 \leq u_2(t) \leq 0.01$, with $W_1 = 0.1$ and $W_2 = 1000$. We assumed $u_2(t)$ will be significantly affected by changes on the bounds of the controls compared to $u_1(t)$, hence, we adjusted W_2 from 100 to 1000 while W_1 remains 0.1. Under this scenario, we noted that the total number of new infections generated in human and animal populations in the presence of controls over 2000 days will be $T_h = 482$ and $T_a = 544$, respectively, implying that optimal control strategies will be responsible for averting approximately 4,053 and 1,927 infections in human and animal populations, respectively. Thus, relative to the total number of infections in the absence of controls, the presence of controls will be associated with 89.4% and 78% reductions for human and animal

populations, respectively. Comparing with earlier scenarios (Figures 1 and 3), we can see that this scenario will have more impact on disease management. In addition, the control profiles associated with this scenario (Figure 6) suggests that for these results to be attained, control $u_1(t)$ will have to be maintained at its maximum intensity from the start to the final day, while control $u_2(t)$ can be maintained at maximum intensity from the start and can be ceased immediately after 500th day of implementation. Thus at higher costs and intensity, control $u_2(t)$ cannot be maintained at its maximum intensity from the start till the final day. In addition, the total cost of implementation under this scenario will be $J = 32,559$.

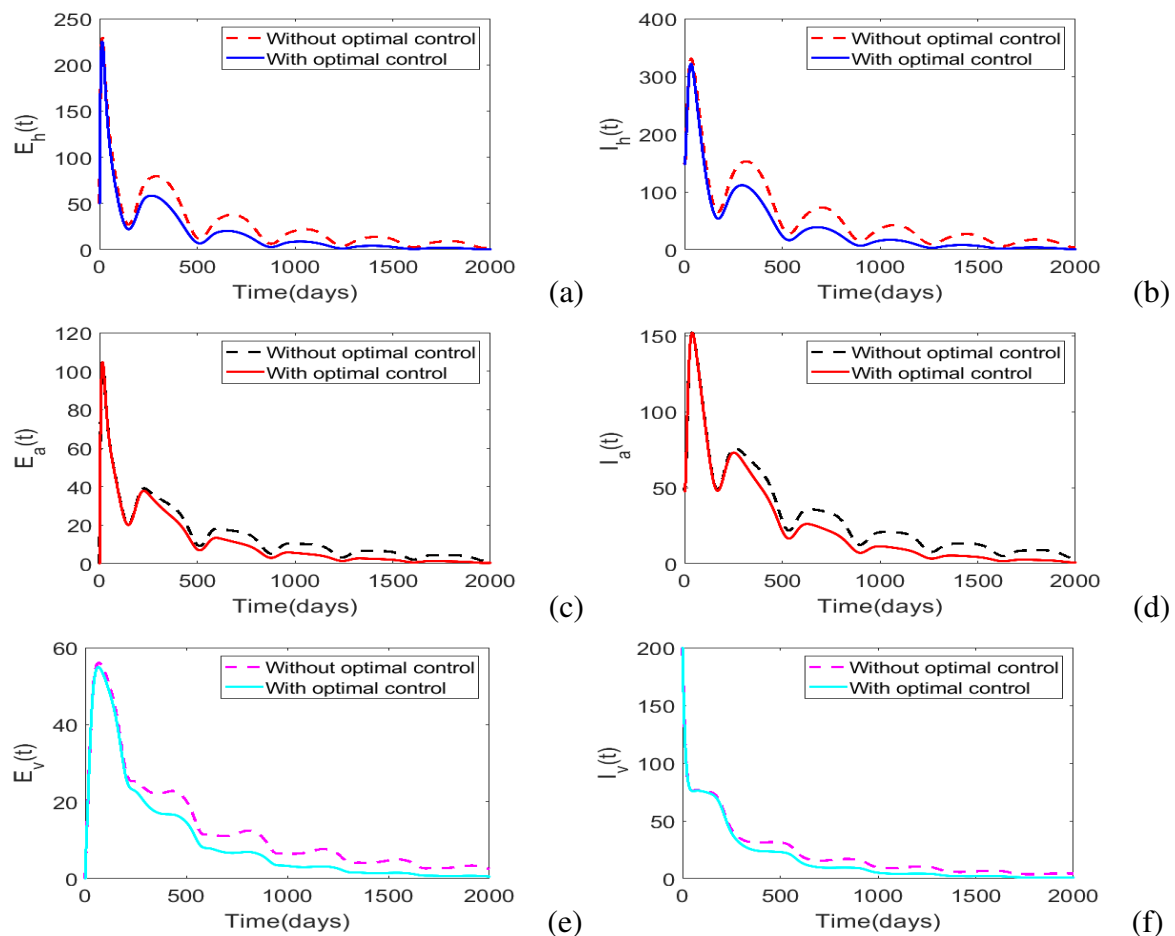


Figure 1. Simulations of model (4) with and without optimal control, with $0 \leq u_1(t) \leq 0.003$ and $u_2(t) = 0$, $W_1 = 0.1$ and $W_2 = 0$. The solid and dotted curves in (a)–(f) depicts the population levels in the host populations with and without optimal control, respectively. Overall, we can observe that with optimal control strategies, the total number of new infections for the hosts is low compared to when there are no optimal control strategies.

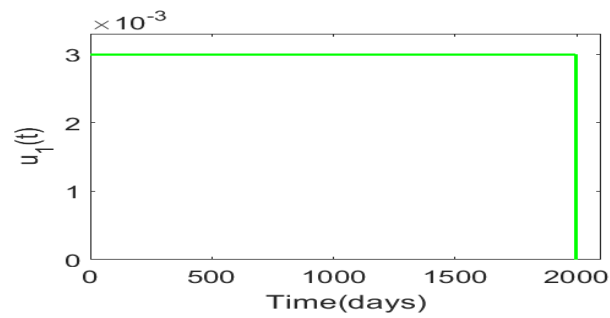


Figure 2. Control profile for $u_1(t)$, ($0 \leq u_1(t) \leq 0.03$), $u_2(t) = 0$ and $w_1 = 0.1$. We can see that for effective disease management, control $u_1(t)$ will have to be maintained at its maxima for the entire time horizon.

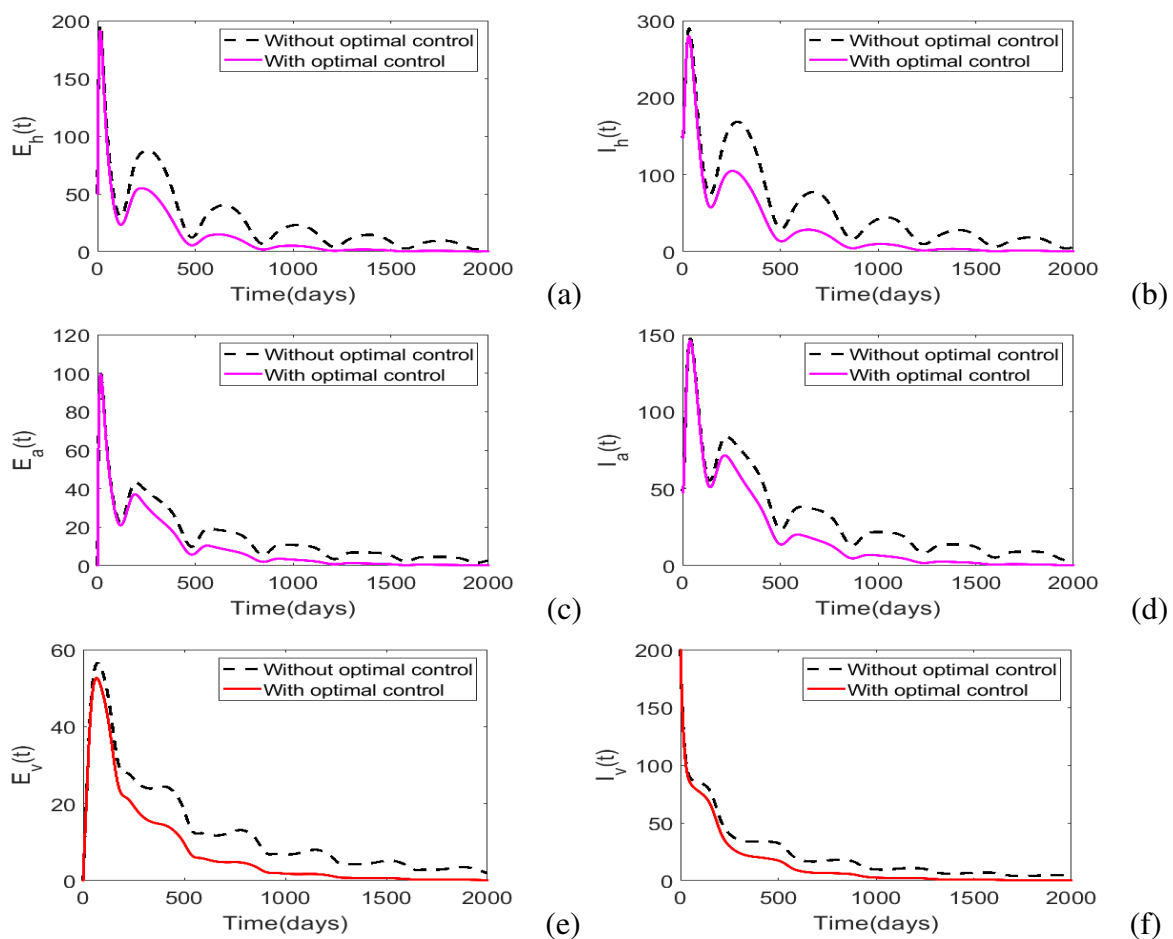


Figure 3. Simulations of model (4) with and without optimal human awareness and insecticides use over 2000 days. We set $0 \leq u_1(t) \leq 0.003$, $0 \leq u_2(t) \leq 0.001$, $W_1 = 0.1$ and $W_2 = 100$. We assume that insecticides use is more expensive relative to human awareness campaigns, hence $W_1 < W_2$. The solid and dotted curves in (a)–(f) represent the population levels in the host populations with and without optimal control, respectively.

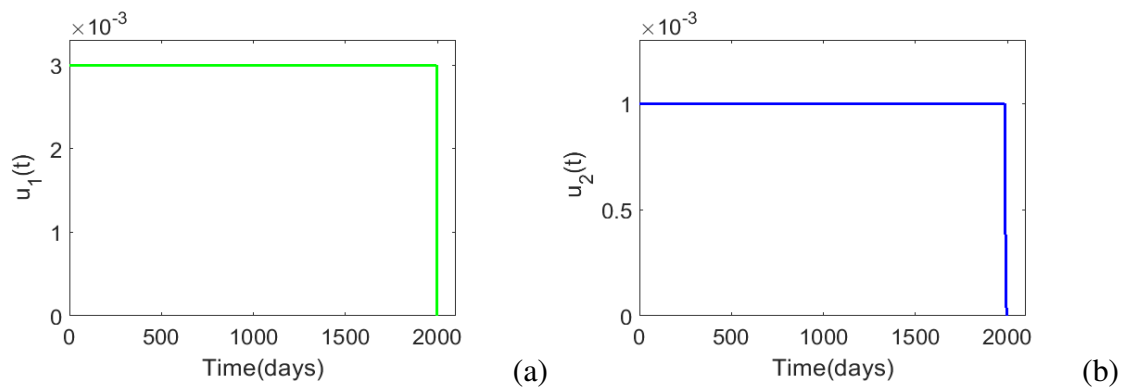


Figure 4. Numerical results illustrating the control profiles for $u_1(t)$, ($0 \leq u_1(t) \leq 0.003$) and $u_2(t)$ ($0 \leq u_2(t) \leq 0.001$), with $W_1 = 0.1$ and $W_2 = 100$. The results suggests that for effective disease management both controls need to be maintained at their respective maxima for the entire time horizon.

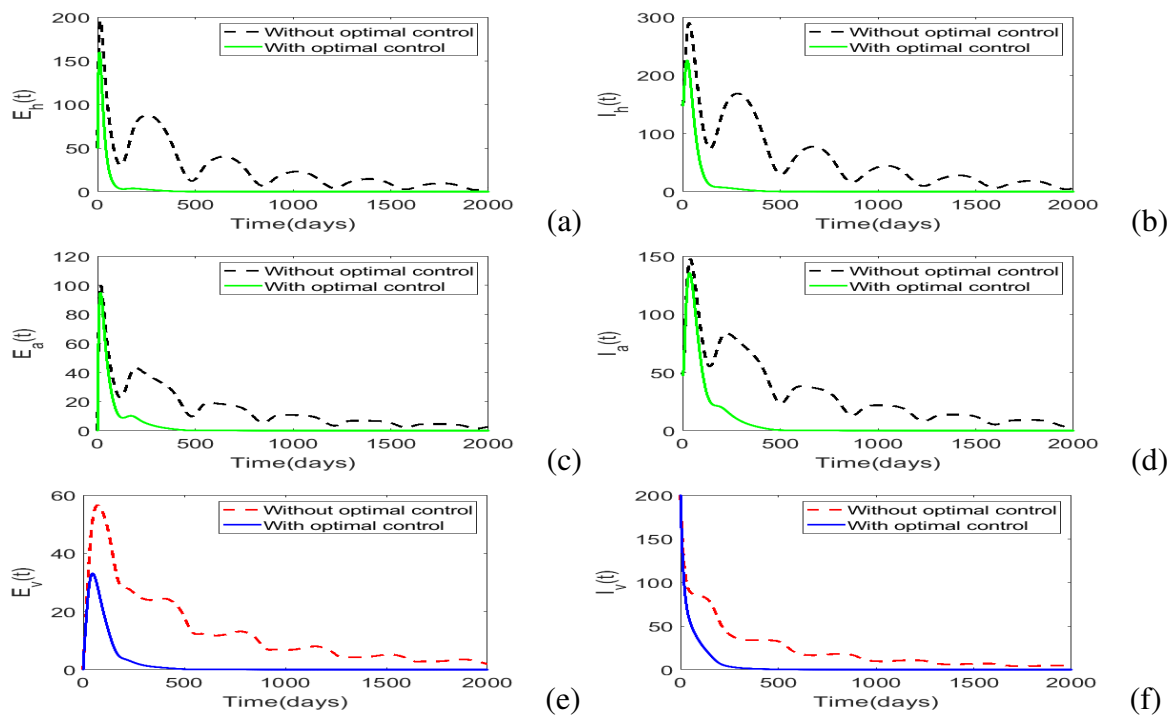


Figure 5. Simulations of model (4) with and without optimal human awareness and insecticides use over 2000 days. We set $0 \leq u_1(t) \leq 0.03$, $0 \leq u_2(t) \leq 0.01$, $W_1 = 0.1$ and $W_2 = 1000$. Once again, we assume that insecticides use is more expensive compared to human awareness campaigns, hence $W_1 < W_2$. The solid and dotted curves in (a)–(f) represent the population levels in the host populations with and without optimal control, respectively.

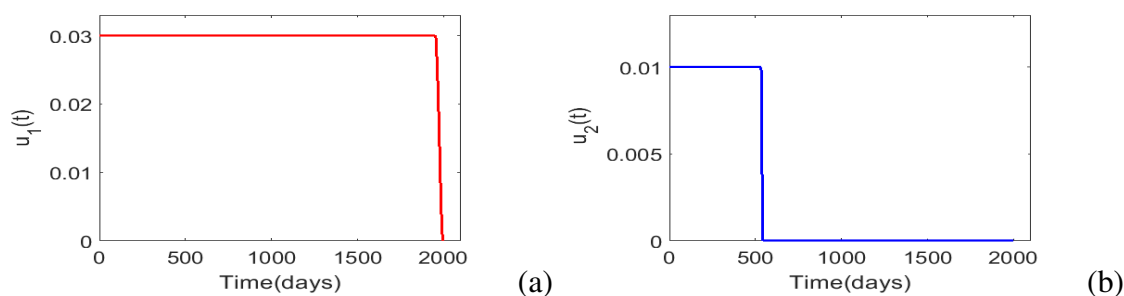


Figure 6. Numerical results illustrating the control profiles for $u_1(t)$, ($0 \leq u_1(t) \leq 0.03$) and $u_2(t)$ ($0 \leq u_2(t) \leq 0.01$), with $W_1 = 0.1$ and $W_2 = 10^3$. The results suggests that for these weight constants, the human awareness control $u_1(t)$ will have to maintained at its maxima from the start till the end and the insecticide control, $u_2(t)$ need to be implemented at its maxima from the start and can be ceased immediately after 500 days.

3. Discussion and concluding remarks

In this study, a periodic model consisting of two hosts (animals and humans) and the tsetse vector has been proposed and comprehensively analysed with a view to explore the impact of optimal human awareness and insecticides use on transimission and control of *Trypanosoma brucei rhodesiense* in a periodic environment. We computed the basic reproduction number and demonstrated that it is an important threshold quantity for disease persistence and extinction. In particular, we have demonstrated that whenever the basic reproduction number is less than unity then the disease dies out and the reverse occurs whenever it is greater than unity. The main goal of introducing the two controls in the proposed model was necessitated by the desire to identify effective ways of minimizing the number of infected human over time at minimal costs. Hence utilizing optimal control theory several possible outcomes of effectively managing the disease were explored. One of the important outcome from this study was that effective control of the disease can be managed if optimal human awareness campaigns are combined with optimal insecticides use. This result was attained after comparing the strength of optimal human awareness alone and when it is combined with optimal insecticides use. We also made this comparison based on the fact that insecticides use is known to be associated with some adverse effects to the environment. Therefore, this study suggests that by totally eliminating insecticides use from a whole matrix of other *Trypanosoma brucei rhodesiense* intervention strategies may present a formidable challenge on effective disease management. We have also noted that at certain implementation costs, effective management can be attained with low intensity use of insecticides for a shorter period of time.

The proposed model is not exhaustive. In future, we will incorporate the effects of host movement, which is one of the integral factors in transmission and control of *Trypanosoma brucei rhodesiense*.

Acknowledgements

Mlyashimbi Helikumi acknowledges the financial support received from the Mbeya University of Science and Technology, Tanzania. The other authors are also grateful to their respective institutions

for the support.

We would like to thank the three anonymous referees and the editors for their invaluable comments and suggestions.

Conflict of interest

The authors declare that they have no competing interests.

References

1. R. Lowe, The impact of global environmental change on vector-borne disease risk: A modelling study, *Lancet Planet. Health.*, **2** (2018), S1.
2. H. J. Nnko, A. Ngonyoka, L. Salekwa, A. B. Estes, P. J. Hudson, P. S. Gwakisa, et al. Seasonal variation of tsetse fly species abundance and prevalence of trypanosomes in the Maasai steppe, Tanzania, *J. Vector Ecol.*, **42** (2017), 24–33.
3. J. R. Franco, P. P. Simarro, A. Diarra, J. G. Jannin. Epidemiology of human African trypanosomiasis, *Clin. Epidemiol.*, **6** (2014), 257–275.
4. World Health Organization Report, Control and Surveillance of Human African Trypanosomiasis, 2013. Available from: <https://apps.who.int/iris/handle/10665/95732>.
5. World Health Organization, Human African trypanosomiasis (sleeping sickness): Epidemiological update, *Wkly Epidemiol. Rec.*, **81** (2018), 71–80.
6. S. G. A. Leak, Tsetse vector population dynamics, in *Modelling Vector-Borne and Other Parasitic Diseases* (eds. J. W. Hansen and B.D. Perry), International Livestock research Institute, (1994), 36.
7. F. L. Berrang, C. Wamboga, A. Kakembo, Trypanosoma brucei rhodesiense sleeping sickness, Uganda, *Emerg. Infect. Dis.*, **18** (2012), 1686–1687.
8. K. Ngongolo, A. B. Estes, P. J. Hudson, P. S. Gwakisa, Influence of seasonal cattle movement on prevalence of trypanosome infections in cattle in the Maasai Steppe, Tanzania, *J. Infect. Dis. Epidemiol.*, **5** (2019), 079.
9. E. G. Kimaro, J. L. Toribio, P. Gwakisa, S. M. Mor, Occurrence of trypanosome infections in cattle in relation to season, livestock movement and management practices of Maasai pastoralists in Northern Tanzania, *Vet. Parasitol. Reg. Stud. Reports.*, **12** (2018), 91–98.
10. S. Aksoy, P. Buscher, M. Lehane, P. Solano, J. Van Den Abbeele, Human African trypanosomiasis control: Achievements and challenges, *PLoS Negl. Trop. Dis.*, **11** (2017), e0005454.
11. P. P. Simarro, G. Cecchi, J. R. Franco, M. Paone, A. Diarra, J. A. Ruiz-Postigo, et al., Estimating and mapping the population at risk of sleeping sickness, *PLoS Negl. Trop. Dis.*, **6** (2012), e1859.
12. P. Büscher, G. Cecchi, V. Jamonneau, G. Priotto, Human African trypanosomiasis, *Lancet.*, **390** (2017), 2397–2409.
13. S. Moore, S. Shrestha, K. W. Tomlinson, H. Vuong, Predicting the effect of climate change on African trypanosomiasis: Integrating epidemiology with parasite and vector biology, *J. R. Soc. Interface.*, **9** (2012), 817–830.

14. S. L. Peck, J. Bouyer, Mathematical modeling, spatial complexity, and critical decisions in tsetse control, *J. Econ. Entomol.*, **105** (2012), 1477–1486.
15. J. W. Hargrove, R. Ouifki, D. Kajunguri, G. A. Vale, S. J. Torr, Modeling the control of trypanosomiasis using trypanocides or insecticide-treated livestock, *PLoS Negl. Trop. Dis.*, **6** (2012), e1615.
16. S. F. Ackley, J. W. Hargrove, A dynamic model for estimating adult female mortality from ovarian dissection data for the tsetse fly *Glossina pallidipes* Austen sampled in Zimbabwe, *PLoS Negl. Trop. Dis.*, **11** (2017), e0005813.
17. J. S. Lord, J.W. Hargrove JW, S. J. Torr, G. A. Vale, Climate change and African trypanosomiasis vector populations in Zimbabwe's Zambezi Valley: A mathematical modelling study, *PLoS Med.*, **15** (2018), e1002675.
18. S. Alderton, E. T. Macleod, N. E. Anderson, G. Palmer, N. Machila, M. Simuunza, et al., An agent-based model of tsetse fly response to seasonal climatic drivers: Assessing the impact on sleeping sickness transmission rates, *PLoS Negl. Trop. Dis.*, **12** (2018), e0006188.
19. C. M. Stone, N. Chitnis N, Implications of heterogeneous biting exposure and animal hosts on trypanosomiasis *Brucei Gambiense* transmission and control, *PLoS Comput. Biol.*, **11** (2015): e1004514.
20. D. J. Rogers, A general model for the African trypanosomiasis, *Parasitology.*, **97** (1988), 193–212.
21. K. S. Rock, M. L. Ndeffo-Mbah, S. Castaño, C. Palmer, A. Pandey, K. E. Atkins, et al. Assessing strategies against Gambiense sleeping sickness through mathematical modeling, *Clin. Infect. Dis.*, **66** (2018), S286–S292.
22. A. M. Ndong, J. M. W. Munganga, J. N. Mwambakana, M. C. Saad-Roy, P. van den Driessche, O. R. Walo. Analysis of a model of Gambiense sleeping sickness in human and cattle, *J. Biol. Dyn.*, **10** (2016), 347–365.
23. J. A. Gilbert, J. Medlock, J. P. Townsend, S. Aksoy, M. L. Ndeffo-Mbah, A. P. Galvani, Determinants of human African trypanosomiasis elimination via paratransgenesis, *PLoS Negl. Trop. Dis.*, **10** (2016), e0004465.
24. K. S. Rock, S. J. Torr, C. Lumbala, M. J. Keeling, Predicting the impact of intervention strategies for sleeping sickness in two high-endemicity health zones of the Democratic Republic of Congo, *PLoS Negl. Trop. Dis.*, **11** (2017), e0005162.
25. K. S. Rock, S. J. Torr, C. Lumbala, M. J. Keeling, Quantitative evaluation of the strategy to eliminate human African trypanosomiasis in the Democratic Republic of Congo, *Parasit. Vectors.*, **8** (2015), 532.
26. K. S. Rock, C. M. Stone, I. M. Hastings, M. J. Keeling, S. J. Torr, N. Chitnis, Mathematical models of human African trypanosomiasis epidemiology, *Adv. Parasitol.*, **87** (2015), 53–133.
27. T. Madsen, D. I. Wallace, N. Zupan, Seasonal fluctuations in tsetse fly populations and human African trypanosomiasis: A mathematical model, in *BiIOMAT 2012: International Symposium on Mathematical and Computational Biology* (ed. R. P. Mondaini), World Scientific Publishing Company, Singapore, (2013), 56–69.

28. H. Helikumi, M. Kgosimore, D. Kuznetsov, S. Mushayabasa S, Backward bifurcation and optimal control analysis of a *Trypanosoma Brucei Rhodesiense* model, *Mathematics.*, **7** (2019), 971.
29. A. R. Cossins, K. Blower, *Temperature biology of animals*, New York, Chapman and Hall, 1987.
30. N. Chitnis, J. M. Cushing, J. M. Hyman, Bifurcation analysis of a mathematical model for malaria transmission, *SIAM J. Appl. Math.*, **67** (2006), 24–45.
31. N. Chitnis, J. M. Hyman, J. M. Cushing, Determining important parameters in the spread of malaria through the sensitivity analysis of a mathematical model, *Bull. Math. Biol.*, **70** (2008), 1272–1296.
32. P. van den Driessche, J. Watmough, Reproduction numbers and sub-threshold endemic equilibria for compartmental models of disease transmission, *Math. Biosci.*, **180** (2002), 29–48.
33. L. S. Pontryagin, V. T. Boltyanskii, R. V. Gamkrelidze, E. F. Mishcheuko, *The mathematical theory of optimal processes*, Wiley, New Jersey, 1962.
34. S. Lenhart, J. T. Workman, *Optimal Control Applied to Biological Models*, Chapman and Hall/CRC, London, 2007.
35. W. Wang, X. Q. Zhao, Threshold dynamics for compartment epidemic models in periodic environments, *J. Dyn. Differ. Equ.*, **20** (2008), 699–717.
36. D. Posny, J. Wang, Computing basic reproductive numbers for epidemiological models in non-homogeneous environments, *Appl. Math. Comput.*, **242** (2014), 473–490.
37. W. D. Wang, X. Q. Zhao, An epidemic model in a patchy environment, *Math. Biosci.*, **190** (2004), 97–112.
38. X. Q. Zhao, *Dynamical System in Population Biology*, Springer-Verlag, New York, 2003.
39. X. Q. Zhao, *Dynamical Systems in Population Biology*, Springer: New York, 2003.
40. W. H. Fleming, R. W. Rishel, *Deterministic and Stochastic Optimal Control*, Springer-Verag, New York, 1975.

Supplementary

Appendix A. Positivity and boundedness of solutions

Theorem 1. *The solutions $(S_h(t), E_h(t), I_h(t), R_h(t), S_a(t), E_a(t), I_a(t), R_a(t), S_v(t), E_v(t), I_v(t))$ of the model (3) are uniformly and ultimately bounded in*

$$\Omega = \left\{ \begin{array}{l} \left(\begin{array}{l} S_h(t) + E_h(t) + I_h(t) + R_h(t) \\ S_a(t) + E_a(t) + I_a(t) + R_a(t) \\ S_v(t) + E_v(t) + I_v(t) \end{array} \right) \in \mathbb{R}_+^{11} \left| \begin{array}{l} N_h(t) \leq N_{h0}, \\ N_a(t) \leq N_{a0}, \\ N_v(t) \leq N_{v0} \end{array} \right. \right\},$$

with $N_h(0) = N_{h0}$, $N_a(0) = N_{a0}$ and $N_v(0) = N_{v0}$.

Proof. For the *Trypanosoma brucei rhodesiense* model (3) to be epidemiologically meaningful, it is important to demonstrate that all its state variables are non-negative for all $t \geq 0$. In other words, one needs to show that solutions of system (3) with non-negative initial data will remain non-negative for

all $t \geq 0$. Let the initial data $S_i(0) \geq 0$, $E_i(0) \geq 0$, $I_i(0) \geq 0$, $R_i(0) \geq 0$, for $i = a, h$, and $S_v(0) \geq 0$, $E_v(0) \geq 0$, and $I_v(0) \geq 0$, such that from the second equation of model (3) we have

$$E_h(t) = e^{-(\mu_h + \kappa_h)t} \left(E_h(0) + \int_0^t \lambda_h(s) S_h(s) ds \right), \quad t \geq 0.$$

Thus, $E_h(t) \geq 0$ for all $t \geq 0$. A similar approach can be utilised to show that all the other variables of model (3) are positive for all $t \geq 0$. In what follows, we now determine the feasible region of model (3). One can easily verify the that rate of change of the total host populations N_i , ($i = a, h$) is

$$N_i'(t) = (b_i - \mu_i)N_i(t) - d_i I_i(t) \leq (b_i - \mu_i)N_i(t), \quad \text{where} \quad \mu_i \leq b_i.$$

As suggested in [13] we set $b_i = \mu_i$, otherwise the population will grow without bound or become extinct. Therefore, $N_i(t) \leq N_i(0)$. Similarly, by adding all the last three equations of model (3), and setting $b_v(t) = \mu_v(t)$ as in [13], one gets $N(t) \leq N_{v0}$. Thus, model (3) is epidemiologically and mathematically well-posed in the domain:

$$\Omega = \left\{ \begin{array}{l} \left(\begin{array}{l} S_h(t) + E_h(t) + I_h(t) + R_h(t) \\ S_a(t) + E_a(t) + I_a(t) + R_a(t) \\ S_v(t) + E_v(t) + I_v(t) \end{array} \right) \in \mathbb{R}_+^{11} \left| \begin{array}{l} N_h(t) \leq N_{h0}, \\ N_a(t) \leq N_{a0}, \\ N_v(t) \leq N_{v0} \end{array} \right. \right\},$$

with $N_h(0) = N_{h0}$, $N_a(0) = N_{a0}$ and $N_v(0) = N_{v0}$. This completes the proof of theorem. \square

Appendix B. Extinction and uniform persistence of the disease

Before we investigate the extinction and persistence of the disease, we need to determine the basic reproduction number of the model. Commonly denoted by \mathcal{R}_0 , the basic reproduction number is an epidemiologically important threshold value which determines the ability of an infectious disease invading a population. To determine the reproduction number of model (3), the next-generation matrix method [32] will be utilized. One can easily verify that model (3) has a disease-free equilibrium $\mathcal{E}^0 : (S_h^0, E_h^0, I_h^0, R_h^0, S_a^0, E_a^0, I_a^0, R_a^0, S_v^0, E_v^0, I_v^0) = (N_{h0}, 0, 0, 0, 0, N_{a0}, 0, 0, 0, N_{v0}, 0, 0)$.

The infected compartments of model (3) is comprised of $(E_j(t), I_j(t))$ classes, for $j = h, a, v$. Following the next-generation matrix approach, the nonnegative matrix $F(t)$ of the infection terms and the non-singular matrix, $V(t)$ of the transition terms evaluated at \mathcal{E}^0 are,

$$F(t) = \begin{bmatrix} 0 & 0 & 0 & 0 & 0 & \frac{\sigma_v(t)\sigma_h\beta_{vh}N_{h0}}{\sigma_v(t)N_v(t) + \sigma_h N_{h0}} \\ 0 & 0 & 0 & 0 & 0 & 0 \\ 0 & 0 & 0 & 0 & 0 & \frac{\sigma_v(t)\sigma_a\beta_{va}N_{a0}}{\sigma_v(t)N_v(t) + \sigma_a N_{a0}} \\ 0 & 0 & 0 & 0 & 0 & 0 \\ 0 & \frac{\sigma_h\sigma_v(t)\beta_{hv}N_v(t)}{\sigma_v(t)N_v(t) + \sigma_h N_{h0}} & 0 & \frac{\sigma_a\sigma_v(t)\beta_{va}N_v(t)}{\sigma_v(t)N_v(t) + \sigma_a N_{a0}} & 0 & 0 \\ 0 & 0 & 0 & 0 & 0 & 0 \end{bmatrix},$$

and

$$V(t) = \begin{bmatrix} \kappa_h + \mu_h & 0 & 0 & 0 & 0 & 0 \\ -\kappa_h & \mu_h + \alpha_h + d_h & 0 & 0 & 0 & 0 \\ 0 & 0 & \kappa_a + \mu_a & 0 & 0 & 0 \\ 0 & 0 & -\kappa_a & \mu_a + \alpha_a + d_a & 0 & 0 \\ 0 & 0 & 0 & 0 & \kappa_v(t) + \mu_v(t) & 0 \\ 0 & 0 & 0 & 0 & -\kappa_v(t) & \mu_v(t) \end{bmatrix}. \quad (6)$$

Therefore, the basic reproduction number of the time-averaged autonomous system is

$$[\mathcal{R}_0] = \sqrt{\mathcal{R}_{0h} + \mathcal{R}_{0a}},$$

where

$$\mathcal{R}_{0h} = \left(\frac{\kappa_h \beta_{vh} N_{h0} \kappa_{v0} \beta_{hv} N_{v0}}{\mu_{v0}(\kappa_{v0} + \mu_{v0})(\kappa_h + \mu_h)(\mu_h + \alpha_h + d_h)} \right) \left(\frac{\sigma_h \sigma_{v0}}{\sigma_{v0} N_{v0} + \sigma_h N_{h0}} \right)^2,$$

$$\mathcal{R}_{0a} = \left(\frac{\kappa_a \beta_{va} N_{a0} \kappa_{v0} \beta_{av} N_{v0}}{\mu_{v0}(\kappa_{v0} + \mu_{v0})(\kappa_a + \mu_a)(\mu_a + \alpha_a + d_a)} \right) \left(\frac{\sigma_a \sigma_{v0}}{\sigma_{v0} N_{v0} + \sigma_a N_{a0}} \right)^2.$$

In order to define the basic reproduction number of this non-autonomous model, we follow the work of Wang and Zhao [35]. They introduced the next-infection operator L for a model in periodic environments by

$$(L\phi)(t) = \int_0^\infty Y(t, t-s) F(t-s) \phi(t-s) ds,$$

where $Y(t, s)$, $t \geq s$, is the evolution operator of the linear ω -periodic system $\frac{dy}{dt} = -V(t)y$ and $\phi(t)$, the initial distribution of infectious animals, is ω -periodic and always positive. The effective reproductive number for a periodic model is then determined by calculating the spectral radius of the next infection operator,

$$\mathcal{R}_0 = \rho(L). \quad (7)$$

For model (3), the evolution operator can be determined by solving the system of differential equations $\frac{dy}{dt} = -V(t)y$ with the initial condition $Y(s, s) = I_{6 \times 6}$; thus, one gets

$$Y(t, s) = \begin{bmatrix} y_{11}(t, s) & 0 & 0 & 0 & 0 & 0 \\ y_{21}(t, s) & y_{22}(t, s) & 0 & 0 & 0 & 0 \\ 0 & 0 & y_{33}(t, s) & 0 & 0 & 0 \\ 0 & 0 & y_{43}(t, s) & y_{44}(t, s) & 0 & 0 \\ 0 & 0 & 0 & 0 & y_{55}(t, s) & 0 \\ 0 & 0 & 0 & 0 & y_{65}(t, s) & e^{-\mu_v(t-s)} \end{bmatrix}.$$

where

$$y_{11}(t, s) = e^{-(\mu_h + \kappa_h)(t-s)},$$

$$\begin{aligned}
y_{21}(t, s) &= \frac{\kappa_h}{d_h + \alpha_h - \kappa_h} \left(e^{-(\mu_h + \kappa_h)(t-s)} - e^{-(\mu_h + d_h + \alpha_h)(t-s)} \right), \\
y_{22}(t, s) &= e^{-(\mu_h + d_h + \alpha_h)(t-s)}, \\
y_{33}(t, s) &= e^{-(\mu_a + \gamma_a)(t-s)}, \\
y_{43}(t, s) &= \frac{\kappa_a}{d_a + \alpha_a - \kappa_a} \left(e^{-(\mu_a + \gamma_a)(t-s)} - e^{-(\mu_a + d_a + \alpha_a)(t-s)} \right), \\
y_{44}(t, s) &= e^{-(\mu_a + d_a + \alpha_a)(t-s)}, \\
y_{55}(t, s) &= \exp \left\{ \kappa_{v0}(t-s) + \frac{2\kappa_{v0}\kappa_{v1}}{\omega} \cos \left(\frac{\omega}{2}(t+\tau+s) \right) \sin \left(\frac{\omega}{2}(t+\tau-s) \right) \right. \\
&\quad \left. + \mu_{v0}(t-s) + \frac{2\mu_{v0}\mu_{v1}}{\omega} \cos \left(\frac{\omega}{2}(t+\tau+s) \right) \sin \left(\frac{\omega}{2}(t-s) \right) \right\}, \\
y_{65}(t, s) &= \left(e^{-\int_s^t \mu_v(x) dx} \right) \int_s^t e^{\mu_v(x)} \kappa_v(x) y_{55}(x, s) dx, \\
y_{66}(t, s) &= \exp \left\{ \mu_{v0}(t-s) + \frac{2\mu_{v0}\mu_{v1}}{\omega} \cos \left(\frac{\omega}{2}(t+\tau+s) \right) \sin \left(\frac{\omega}{2}(t+\tau-s) \right) \right\}.
\end{aligned}$$

Utilising the techniques described in [36] one can numerically analyse the basic reproduction number defined in Eq (7). The following lemma shows that the basic reproduction number \mathcal{R}_0 is the threshold parameter for local stability of the disease-free equilibrium \mathcal{E}^0 .

Lemma 1. (Theorem 2.2 in Wang and Zhao [35]). Let $x(t) = (E_i(t), I_i(t))$, $i = a, h, v$, denote the vector of all infected class variables system (3), such that the linearization of system (3) at disease-free equilibrium \mathcal{E}^0 is

$$\dot{x}(t) = (F(t) - V(t))x(t), \quad (8)$$

where $F(t)$ and $V(t)$ are defined earlier on Eq (6). Furthermore, let $\Phi_{F-V(t)}$ and $\rho(\Phi_{F-V(\omega)})$ be the monodromy matrix of system (8) and the spectral radius of $\Phi_{F-V(t)}(\omega)$, respectively, then the following statements are valid:

- (i) $\mathcal{R}_0 = 1$, if and only if $\rho(\Phi_{F-V(\omega)}) = 1$;
- (ii) $\mathcal{R}_0 > 1$, if and only if $\rho(\Phi_{F-V(\omega)}) > 1$;
- (iii) $\mathcal{R}_0 < 1$, if and only if $\rho(\Phi_{F-V(\omega)}) < 1$.

Thus, the disease-free equilibrium \mathcal{E}^0 of system (3) is locally asymptotically stable if $\mathcal{R}_0 < 1$ and unstable if $\mathcal{R}_0 > 1$.

In what follows, we now demonstrate that the reproduction number \mathcal{R}_0 is an important threshold parameter for disease extinction and persistence. Precisely, we will show that when $\mathcal{R}_0 < 1$, model (3) admits a globally asymptotically stable disease-free equilibrium \mathcal{E}^0 , and if $\mathcal{R}_0 > 1$, the disease persists. The mathematical analysis follows the approach in [37].

Theorem 2. If $\mathcal{R}_0 < 1$, then the disease-free equilibrium \mathcal{E}^0 of system (3) is globally asymptotically stable in Ω .

Proof. According to Lemma 1, if $\mathcal{R}_0 < 1$, then the disease-free equilibrium \mathcal{E}^0 of system (3) is locally asymptotically stable. Hence, it is sufficient to demonstrate that for $\mathcal{R}_0 < 1$, the disease-free equilibrium is the global attractor. Assume that $\mathcal{R}_0 < 1$, again from Lemma 1, we have, we have $\rho(\Phi_{F-V}(\omega)) < 1$. From the second, third, sixth, seventh, tenth and eleventh equations of model (3) we have:

$$\begin{cases} \dot{E}_h(t) \leq \left(\frac{\sigma_v(t)\sigma_h\beta_{vh}I_v}{\sigma_v(t)N_v(t) + \sigma_h N_h} \right) S_h^0 - (\mu_h + \kappa_h)E_h, \\ \dot{I}_h(t) = \kappa_h E_h - (\mu_h + d_h + \alpha_h)I_h, \\ \dot{E}_a(t) \leq \left(\frac{\sigma_v(t)\sigma_a\beta_{va}I_v}{\sigma_v(t)N_v(t) + \sigma_a N_a} \right) S_a^0 - (\mu_a + \kappa_a)E_a, \\ \dot{I}_a(t) = \kappa_a E_a - (\mu_a + d_a + \alpha_a)I_a, \\ \dot{E}_v(t) \leq \left(\frac{\sigma_v(t)\sigma_h\beta_{hv}I_h}{\sigma_v(t)N_v(t) + \sigma_h N_h} + \frac{\sigma_v(t)\sigma_a\beta_{va}I_a}{\sigma_v(t)N_v(t) + \sigma_a N_a} \right) S_v^0 - (\kappa_v(t) + \mu_v(t))E_v, \\ \dot{I}_v(t) = \kappa_v(t)E_v - \mu_v(t)I_v, \end{cases}$$

for $t \geq 0$. Consider the following auxiliary system:

$$\begin{cases} \dot{\tilde{E}}_h(t) = \left(\frac{\sigma_v(t)\sigma_h\beta_{vh}\tilde{I}_v}{\sigma_v(t)\tilde{N}_v + \sigma_h\tilde{N}_h} \right) S_h^0 - (\mu_h + \kappa_h)\tilde{E}_h, \\ \dot{\tilde{I}}_h(t) = \kappa_h\tilde{E}_h - (\mu_h + d_h + \alpha_h)\tilde{I}_h, \\ \dot{\tilde{E}}_a(t) = \left(\frac{\sigma_v(t)\sigma_a\beta_{va}\tilde{I}_v}{\sigma_v(t)\tilde{N}_v + \sigma_a\tilde{N}_a} \right) S_a^0 - (\mu_a + \kappa_a)\tilde{E}_a, \\ \dot{\tilde{I}}_a(t) = \kappa_a\tilde{E}_a(t) - (\mu_a + d_a + \alpha_a)\tilde{I}_a(t), \\ \dot{\tilde{E}}_v(t) = \left(\frac{\sigma_v(t)\sigma_h\beta_{hv}\tilde{I}_h}{\sigma_v(t)\tilde{N}_v(t) + \sigma_h\tilde{N}_h} + \frac{\sigma_v(t)\sigma_a\beta_{va}\tilde{I}_a}{\sigma_v(t)\tilde{N}_v(t) + \sigma_a\tilde{N}_a} \right) S_v^0 - (\kappa_v(t) + \mu_v(t))\tilde{E}_v, \\ \dot{\tilde{I}}_v(t) = \kappa_v(t)\tilde{E}_v - \mu_v(t)\tilde{I}_v. \end{cases}$$

By Lemma 1 and the standard comparison principle, there exist a positive ω -periodic function $\tilde{x}(t)$ such that $x(t) \leq \tilde{x}(t)e^{pt}$, where $\tilde{x}(t) = (\tilde{E}_i(t), \tilde{I}_i(t))^T$, for $i = a, h, v$, and $p = \frac{1}{\omega} \ln \rho(\Phi_{(F-V)(\cdot)}(\omega)) < 0$. Thus we conclude that $x(t) \rightarrow 0$ as $t \rightarrow \infty$, that is,

$$\lim_{t \rightarrow \infty} E_i(t) = 0, \quad \lim_{t \rightarrow \infty} I_i(t) = 0, \quad \lim_{t \rightarrow \infty} R_a(t) = 0, \quad \text{and} \quad \lim_{t \rightarrow \infty} R_h(t) = 0, \quad i = a, h, v.$$

Hence it follows that

$$\lim_{t \rightarrow \infty} S_i(t) = S_i^0, \quad \text{and} \quad \lim_{t \rightarrow \infty} N_h(t) = N_h^0, \quad i = a, h, v.$$

Therefore, the disease-free equilibrium \mathcal{E}^0 of system (3) is globally asymptotically stable. \square

Theorem 3. *If $R_0 > 1$, then system (3) is uniformly persistent, i.e., there exists a positive constant η , such that for all initial values of $(S_i(0), E_i(0), I_i(0), R_k(0)) \in \mathbb{R}_+^5 \times \text{Int}(\mathbb{R}_+)^6$, ($i = a, h, v$, $k = a, h$) the solution of model (3) satisfies:*

$$\liminf_{t \rightarrow \infty} S_i(t) \geq \eta, \quad \liminf_{t \rightarrow \infty} E_i(t) \geq \eta, \quad \liminf_{t \rightarrow \infty} I_i(t) \geq \eta, \quad \liminf_{t \rightarrow \infty} R_k(t) \geq \eta.$$

Proof. Let us define

$$X = \mathbb{R}_+^{11}; \quad X_0 = \mathbb{R}_+^5 \times \text{Int}(\mathbb{R}_+)^6; \quad \partial X_0 = X \setminus X_0.$$

Let $P : X \rightarrow X$ be the Poincaré map associated with our model (3) such that $P(x_0) = u(\omega, x_0) \forall x_0 \in X$, where $u(t, x_0)$ denotes the unique solution of the system with $u(0, x_0) = x_0$.

We begin by demonstrating that P is uniformly persistent with respect to $(X_0, \partial X_0)$. One can easily deduce that from model (3), X and X_0 are positively invariant. Moreover, ∂X_0 is a relatively closed set in X . It follows from Theorem 1 that solutions of model (3) uniformly and ultimately bounded. Thus the semiflow P is point dissipative on \mathbb{R}_+^{11} , and $P : \mathbb{R}_+^{11} \rightarrow \mathbb{R}_+^{11}$ is compact. By Theorem 3.4.8 in [38], it then follows that P admits a global attractor, which attracts every bounded set in \mathbb{R}_+^{11} .

Define

$$M_\partial = \{(S_i(0), E_i(0), I_i(0), R_k(0)) \in \partial X_0 : P^m(S_i(0), E_i(0), I_i(0), R_k(0)) \in \partial X_0, \forall m \geq 0\},$$

for $i = a, h, v, \quad k = a, h$.

Next, we claim that $M_\partial = \{(S_h(0), 0, 0, R_h(0), S_a(0), 0, 0, R_a(0), S_v(0), 0, 0) : S_i \geq 0, R_k \geq 0\}$. Clearly, $\bar{M} = \{(S_h(0), 0, 0, R_h(0), S_a(0), 0, 0, R_a(0), S_v(0), 0, 0) : S_i \geq 0, R_k \geq 0\} \subseteq M_\partial$.

Now, for any $(S_i(0), E_i(0), I_i(0), R_k(0)) \in \partial X_0 \setminus \bar{M}$; if $E_h(0) = I_h(0) = 0$, it follows that $S_i(0) > 0$, $R_h(0) > 0$, $E_a(0) > 0$, $I_a(0) > 0$, $R_a(0) > 0$, $E_v(0) > 0$, $I_v(0) > 0$, $\dot{E}_h(0) = \lambda_h(0)S_h(0) > 0$, and $\dot{I}_h(0) = 0$. If $E_a(0) = I_a(0) = 0$, it follows that $S_i(0) > 0$, $E_h(0) > 0$, $I_h(0) > 0$, $R_h(0) > 0$, $R_a(0) = 0$, $E_v(0) > 0$, $I_v(0) > 0$, $\dot{E}_a(0) = \lambda_a(0)S_a(0) > 0$, and $\dot{I}_a(0) = 0$. If $E_v(0) = I_v(0) = 0$, it follows that $S_i(0) > 0$, $E_h(0) = 0$, $I_h(0) = 0$, $R_h(0) > 0$, $E_a(0) = 0$, $I_a(0) = 0$, $R_a(0) = 0$, $\dot{E}_v(0) = 0$, and $\dot{I}_a(0) = 0$. Thus, we have $(S_i(0), E_i(0), I_i(0), R_k(0)) \notin \partial X_0$ for $0 < t \ll 1$. By the positive invariance of X_0 , we know that $P^m(S_i(0), E_i(0), I_i(0), R_k(0)) \notin \partial X_0$ for $m \geq 1$, hence $(S_i(0), E_i(0), I_i(0), R_k(0)) \notin M_\partial$, and thus $M_\partial = \{(S_h(0), 0, 0, R_h(0), S_a(0), 0, 0, R_a(0), S_v(0), 0, 0) : S_i \geq 0, R_k \geq 0\}$.

Now consider the fixed point $M_0 = (S_h^0, 0, 0, R_h^0, S_a^0, 0, 0, 0, S_v^0, 0, 0)$ of the Poincaré map P , where and define $W^S(M_0) = \{x_0 : P^m(x_0) \rightarrow M_0, m \rightarrow \infty\}$. We show that

$$W^S(M_0) \cap X_0 = \emptyset. \quad (9)$$

Based on the continuity of solutions with respect to the initial conditions, for any $\epsilon > 0$, there exists $\delta > 0$ small enough such that for all $(S_i(0), E_i(0), I_i(0), R_k(0)) \in X_0$ with $\|(S_i(0), E_i(0), I_i(0), R_k(0)) - M_0\| \leq \delta$, we have

$$\|u(t, (S_i(0), E_i(0), I_i(0), R_k(0)) - u(t, M_0)\| < \epsilon, \quad \forall t \in [0, \omega].$$

To obtain (9), we claim that

$$\limsup_{m \rightarrow \infty} \|P^m(S_i(0), E_i(0), I_i(0), R_k(0)) - M_0\| \geq \delta, \quad \forall (S_i(0), E_i(0), I_i(0), R_k(0)) \in X_0.$$

We prove this claim by contradiction; that is, we suppose $\limsup_{m \rightarrow \infty} \|P^m(S_i(0), E_i(0), I_i(0), R_k(0)) - M_0\| < \delta$ for some $(S_i(0), E_i(0), I_i(0), R_k(0)) \in X_0$. Without loss of generality, we assume that $\|P^m(S_i(0), E_i(0), I_i(0), R_k(0)) - M_0\| < \delta, \quad \forall m \geq 0$. Thus,

$$\|u(t, P^m(S_i(0), E_i(0), I_i(0), R_k(0)) - u(t, M_0)\| < \epsilon, \quad \forall t \in [0, \omega] \text{ and } m \geq 0.$$

Moreover, for any $t \geq 0$, we write $t = t_0 + q\omega$ with $t_0 \in [0, \omega)$ and $q = [\frac{t}{\omega}]$, the greatest integer less than or equal to $\frac{t}{\omega}$. Then we obtain

$$\|u(t, (S_i(0), E_i(0), I_i(0), R_k(0))) - u(t, M_0)\| = \|u(t_0, P^m(S_i(0), E_i(0), I_i(0), R_k(0))) - u(t_0, M_0)\| < \epsilon$$

for any $t \geq 0$. Let $(S_i(t), E_i(t), I_i(t), R_k(t)) = u(t, (S_i(0), E_i(0), I_i(0), R_k(0)))$. It follows that $N_{i0} - \epsilon < S_i(t) < N_{i0} + \epsilon$, $0 < E_i(t) < \epsilon$, $0 < I_i(t) < \epsilon$, and $0 < R_k(t) < \epsilon$. Then from the second equation of system (3) we have

$$\begin{aligned} \frac{dE_h}{dt} &= \frac{\sigma_v(t)\sigma_h\beta_{vh}I_vS_h}{\sigma_v(t)N_v + \sigma_hN_h} - (\mu_h + \kappa_h)E_h, \\ &\geq \frac{\sigma_v(t)\sigma_h\beta_{vh}I_v(N_{h0} - \epsilon)}{\sigma_v(t)(N_{v0} + \epsilon) + \sigma_h(N_{h0} + \epsilon)} - (\mu_h + \kappa_h)E_h, \\ &= \left(\frac{\sigma_v(t)\sigma_h\beta_{vh}N_{h0}}{\sigma_v(t)N_{v0} + \sigma_hN_{h0}} \right) \left(1 - \frac{2\epsilon\sigma_h \left(1 + \frac{\sigma_v(t)}{2\sigma_h} + \frac{\sigma_v(t)N_{v0}}{2\sigma_hN_{h0}} \right)}{\sigma_v(t)(N_{v0} + \epsilon) + \sigma_h(N_{h0} + \epsilon)} \right) I_v - (\mu_h + \kappa_h)E_h, \end{aligned}$$

Recall that the third equation of system (3) has the form

$$\dot{I}_h(t) = \kappa_h E_h(t) - (\mu_h + \alpha_h + d_h)I_h.$$

From the sixth equation of system (3) we have

$$\begin{aligned} \frac{dE_a}{dt} &\geq \frac{\sigma_v(t)\sigma_a\beta_{va}I_v(N_{a0} - \epsilon)}{\sigma_v(t)(N_{v0} + \epsilon) + \sigma_h(N_{a0} + \epsilon)} - (\mu_a + \kappa_a)E_a, \\ &= \left(\frac{\sigma_v(t)\sigma_a\beta_{va}N_{a0}}{\sigma_v(t)N_{v0} + \sigma_hN_{a0}} \right) \left(1 - \frac{2\epsilon\sigma_a \left(1 + \frac{\sigma_v(t)}{2\sigma_a} + \frac{\sigma_v(t)N_{v0}}{2\sigma_aN_{a0}} \right)}{\sigma_v(t)(N_{v0} + \epsilon) + \sigma_h(N_{a0} + \epsilon)} \right) I_v - (\mu_a + \kappa_a)E_a, \end{aligned}$$

The seventh equation of system (3) has the form

$$\dot{I}_a(t) = \kappa_a E_a - (\mu_a + \alpha_a + d_a)I_a.$$

The ninth equation of system (3) satisfies

$$\begin{aligned} \frac{dE_v}{dt} &\geq \frac{\sigma_v(t)\sigma_h\beta_{hv}I_h(N_{v0} - \epsilon)}{\sigma_v(t)(N_{v0} + \epsilon) + \sigma_h(N_{h0} + \epsilon)} + \frac{\sigma_v(t)\sigma_a\beta_{av}I_a(N_{v0} - \epsilon)}{\sigma_v(t)(N_{v0} + \epsilon) + \sigma_a(N_{a0} + \epsilon)} - (\mu_v(t) + \kappa_v(t))E_v, \\ &= + \left(\frac{\sigma_v(t)\sigma_h\beta_{hv}N_{v0}}{\sigma_v(t)N_{v0} + \sigma_hN_{h0}} \right) \left(1 - \frac{2\epsilon\sigma_v(t) \left(1 + \frac{\sigma_h}{2\sigma_v(t)} + \frac{\sigma_hN_{h0}}{2\sigma_v(t)N_{v0}} \right)}{\sigma_v(t)(N_{v0} + \epsilon) + \sigma_h(N_{h0} + \epsilon)} \right) I_h \\ &\quad + \left(\frac{\sigma_v(t)\sigma_a\beta_{av}N_{v0}}{\sigma_v(t)N_{v0} + \sigma_aN_{a0}} \right) \left(1 - \frac{2\epsilon\sigma_v(t) \left(1 + \frac{\sigma_a}{2\sigma_v(t)} + \frac{\sigma_aN_{a0}}{2\sigma_v(t)N_{v0}} \right)}{\sigma_v(t) \left(\frac{\Lambda_v}{\mu_v(t)} + \epsilon \right) + \sigma_a(N_{a0} + \epsilon)} \right) I_a - (\mu_v(t) + \kappa_v(t))E_v(t). \end{aligned}$$

Recall that the tenth equation of system (3) has the form

$$\dot{I}_v(t) = \kappa_v(t)E_v - \mu_v(t)I_v.$$

Let

$$M_\epsilon = \begin{bmatrix} 0 & 0 & 0 & 0 & 0 & \frac{2\epsilon\sigma_h\left(1 + \frac{\sigma_v(t)}{2\sigma_h} + \frac{\sigma_v(t)N_{h0}}{2\sigma_h N_{h0}}\right)}{\sigma_v(t)(N_{v0} + \epsilon) + \sigma_h(N_{h0} + \epsilon)} \\ 0 & 0 & 0 & 0 & 0 & 0 \\ 0 & 0 & 0 & 0 & 0 & \frac{2\epsilon\sigma_a\left(1 + \frac{\sigma_v(t)}{2\sigma_a} + \frac{\sigma_v(t)N_{a0}}{2\sigma_a N_{a0}}\right)}{\sigma_v(t)(N_{v0} + \epsilon) + \sigma_a(N_{a0} + \epsilon)} \\ 0 & 0 & 0 & 0 & 0 & 0 \\ 0 & \frac{2\epsilon\sigma_v(t)\left(1 + \frac{\sigma_h}{2\sigma_v(t)} + \frac{\sigma_h N_{h0}}{2\sigma_v(t)N_{v0}}\right)}{\sigma_v(t)(N_{v0} + \epsilon) + \sigma_h(N_{h0} + \epsilon)} & 0 & \frac{2\epsilon\sigma_v(t)\left(1 + \frac{\sigma_a}{2\sigma_v(t)} + \frac{\sigma_a N_{a0}}{2\sigma_v(t)N_{v0}}\right)}{\sigma_v(t)\left(\frac{\Lambda_v}{\mu_v(t)} + \epsilon\right) + \sigma_a(N_{a0} + \epsilon)} & 0 & 0 \\ 0 & 0 & 0 & 0 & 0 & 0 \end{bmatrix},$$

such that

$$[\dot{E}_h, \dot{I}_h, \dot{E}_a, \dot{I}_a, \dot{E}_v, \dot{I}_v]^T \geq [F - V - M_\epsilon][E_h, I_h, E_a, I_a, E_v, I_v]^T.$$

Again based on ([35], Theorem 2.2), we know that if $\rho(\Phi_{F-V}(\omega)) > 1$, then we can choose ϵ small enough such that $\rho(\Phi_{F-V-M_\epsilon}(\omega)) > 1$. Again by ([35], Theorem 2.2) and the standard comparison principle, there exists a positive ω -periodic function $v(t)$ such that $x(t) \geq \tilde{x}_1(t)e^{p_1 t}$, where $\tilde{x}_1(t) = (\tilde{E}_i(t), \tilde{I}_i(t))^T$, for $i = a, h, v$, and $p_1 = \frac{1}{\omega} \ln \rho(\Phi_{F-V-M_\epsilon}(\omega)) > 0$ which implies that

$$\lim_{t \rightarrow \infty} E_i(t) = \infty, \quad \text{and} \quad \lim_{t \rightarrow \infty} I_i(t) = \infty, \quad i = a, h, v.$$

which is a contradiction in M_∂ since M_∂ converges to M_0 . and M_0 is acyclic in M_∂ . By ([39], Theorem 1.3.1), for a stronger repelling property of ∂X_0 , we conclude that P is uniformly persistent with respect to $(X_0, \partial X_0)$, which implies the uniform persistence of the solutions of system (3) with respect to $(X_0, \partial X_0)$ ([39], Theorem 3.1.1). It follows from Theorem 3.1.1 in [39] that the solution of (3) is uniformly persistent. □

Appendix C. Optimal control framework

In this section, an optimal control problem for a seasonal *Trypanosoma brucei rhodesiense* model (4) is formulated and analysed. The main goal being to minimize the population of infected humans at minimal cost of implementation. We define our objective functional as follows

$$J(u_1(t), u_2(t)) = \int_0^{t_f} \left(C_1 I_h(t) + C_2 I_a(t) + \frac{W_1}{2} u_1^2(t) + \frac{W_2}{2} u_2^2(t) \right) dt. \tag{10}$$

The optimal control problem becomes seeking an optimal functions, $U^* = (u_1^*(t), u_2^*(t))$, such that

$$J(u_1^*(t), u_2^*(t)) = \inf_{(u_1, u_2) \in U} J(u_1(t), u_2(t)),$$

for the admissible set $U = \{(u_1(t), u_2(t)) \in (L^\infty(0, t_f))^2 : 0 \leq u_i(t) \leq q_i; q_i \in \mathbb{R}^+, i = 1, 2\}$, where q_i denotes the upper bound of the controls.

In what follows, we investigate the existence of an optimal control pair basing our analysis on the work of Fleming and Rishel (1975) [40]. Based on Theorem 1 we are now aware that all the variables of system (4) have a lower and upper bounds.

Theorem 4. *There exists an optimal control U^* to the problem (4).*

Proof. Suppose that $\mathbf{f}(t, \mathbf{x}, \mathbf{u})$ be the right-hand side of the (4) where by $\mathbf{x} = (S_h, E_h, I_h, R_h, S_a, E_a, I_a, R_a, S_v, E_v, I_v)$ and $\mathbf{u} = (u_1(t), u_2(t))$ represent the vector of state variables and control functions respectively. We list the requirements for the existence of optimal control as presented in Fleming and Rishel (1975) [40]:

1. The function \mathbf{f} is of class C^1 and there exists a constant C such that $|\mathbf{f}(t, 0, 0)| \leq C$, $|\mathbf{f}_x(t, \mathbf{x}, \mathbf{u})| \leq C(1 + |\mathbf{u}|)$, $|\mathbf{f}_u(t, \mathbf{x}, \mathbf{u})| \leq C$;
2. the admissible set of all solutions to system (4) with corresponding control in Ω is nonempty;
3. $\mathbf{f}(t, \mathbf{x}, \mathbf{u}) = \mathbf{a}(t, \mathbf{x}) + \mathbf{b}(t, \mathbf{x})\mathbf{u}$;
4. the control set $U = [0, u_{1\max}] \times [0, u_{2\max}]$ is closed, convex and compact;
5. the integrand of the objective functional is convex in U .

In order to verify these conditions we write

$$\mathbf{f}(t, \mathbf{x}, \mathbf{u}) = \begin{bmatrix} b_h N_h(t) - \lambda_h(t) S_h(t) - \mu_h S_h(t) - u_1(t) S_h(t) + \gamma_h R_h(t) \\ \lambda_h(t) S_h(t) - (\mu_h + \kappa_h) E_h(t) \\ \kappa_h E_h(t) - (\mu_h + \alpha_h + d_h) I_h(t) \\ u_1(t) S_h(t) + \alpha_h I_h(t) - (\mu_h + \gamma_h) R_h(t) \\ b_a N_a(t) - \lambda_a(t) S_a(t) - \mu_a S_a(t) + \gamma_a R_a(t) \\ \lambda_a(t) S_a(t) - (\mu_a + \kappa_a) E_a(t) \\ \kappa_a E_a(t) - (\mu_a + \alpha_a + d_a) I_a(t) \\ \alpha_a I_a(t) - (\mu_a + \gamma_a) R_a(t) \\ b_v(t) N_v(t) - \lambda_v(t) S_v(t) - (\mu_v(t) + u_2(t)) S_v(t) \\ \lambda_v(t) S_v(t) - (\kappa_v(t) + \mu_v(t) + u_2(t)) E_v(t) \\ \kappa_v(t) E_v(t) - (\mu_v(t) + u_2(t)) I_v(t) \end{bmatrix}. \quad (11)$$

From (11), it is clear that $\mathbf{f}(t, \mathbf{x}, \mathbf{u})$ is of class C^1 and $|\mathbf{f}(t, \mathbf{0}, \mathbf{0})| = 0$. In addition, we have one can easily compute $|\mathbf{f}_x(t, \mathbf{x}, \mathbf{u})|$ and $|\mathbf{f}_u(t, \mathbf{x}, \mathbf{u})|$ and demonstrate that

$$|\mathbf{f}(t, \mathbf{0}, \mathbf{0})| \leq C, \quad |\mathbf{f}_x(t, \mathbf{x}, \mathbf{u})| \leq C(1 + |\mathbf{u}|) \quad |\mathbf{f}_u(t, \mathbf{x}, \mathbf{u})| \leq C.$$

Due to the condition 1, the existence of the unique solution for condition 2 for bounded control is satisfied. On the other hand, the quantity $\mathbf{f}(t, \mathbf{x}, \mathbf{u})$ is expressed as linear function of control variables which satisfy the condition 3. \square

After demonstrating the existence of optimal controls, in what follows, we characterize the optimal control functions by utilizing the Pontryagin's Maximum Principle [33]. Pontryagin's Maximum Principle introduces adjoint functions that allow the state system (4) to be attached to the objective functional, that is, it converts the system (4) into the problem of minimizing the Hamiltonian $H(t)$ given by:

$$\begin{aligned} H(t) = & C_1 I_h(t) + C_2 I_a(t) + \frac{W_1}{2} u_1^2(t) + \frac{W_2}{2} u_2^2(t) + \lambda_1(t) [b_h N_h(t) - \lambda_h(t) S_h(t) - (u_1(t) + \mu_h) S_h(t) + \gamma_h R_h(t)] \\ & + \lambda_2(t) [\lambda_h(t) S_h(t) - (\mu_h + \kappa_h) E_h(t)] + \lambda_3(t) [\kappa_h E_h(t) - (\mu_h + d_h + \alpha_h) I_h(t)] \\ & + \lambda_4(t) [u_1(t) S_h(t) + \alpha_h I_h(t) - (\mu_h + \gamma_h) R_h(t)] + \lambda_5(t) [\Lambda_a - \lambda_a(t) S_a(t) - \mu_a S_a(t) + \gamma_a R_a(t)] \end{aligned}$$

$$\begin{aligned}
& +\lambda_6(t)[b_a N_a(t) - \lambda_a(t)S_a - (\mu_a + \kappa_a)E_a(t)] + \lambda_7(t)[\kappa_a E_a(t) - (\mu_a + d_a + \alpha_a)I_a(t)] \\
& +\lambda_8(t)[\alpha_a I_a(t) - (\mu_a + \gamma_a)R_a(t)] + \lambda_9(t)[b_v(t)N_v(t) - \lambda_v(t)S_v(t) - (\mu_v(t) + u_2(t))S_v(t)] \\
& +\lambda_{10}(t)[\lambda_v(t)S_v - (\mu_v(t) + \kappa_v(t) + u_2(t))E_v(t)] + \lambda_{11}(t)[\kappa_v(t)E_v - (\mu_v(t) + u_2(t))I_v(t)]. \quad (12)
\end{aligned}$$

Note that the first part of the terms in $H(t)$ came from the integrand of the objective functional.

Given an optimal control solution (u^*) and the corresponding state solutions ($S_h, E_h, I_h, R_h, S_a, E_a, I_a, R_a, S_v, E_v, I_v$) there exist adjoint functions $\lambda_i(t)$, ($i = 1, 2, 3, \dots, 11$) [34] satisfying

$$\frac{\partial \lambda_i}{\partial t} = -\frac{\partial H}{\partial \mathbf{x}},$$

with transversality condition $\lambda(t_f) = 0$. Thus the adjoint system is:

$$\begin{aligned}
\frac{d\lambda_1}{dt} &= \lambda_1 \mu_h + u_1(t)(\lambda_1 - \lambda_4) + (\lambda_1 - \lambda_2) \frac{\sigma_v(t) \sigma_h \beta_{vh} I_v}{\sigma_v(t) N_v + \sigma_h N_h} + (\lambda_2 - \lambda_1) \frac{\sigma_v(t) \sigma_h^2 \beta_{vh} I_v S_h}{(\sigma_v(t) N_v + \sigma_h N_h)^2} \\
&\quad + (\lambda_{10} - \lambda_9) \frac{\sigma_v(t) \sigma_h^2 \beta_{hv} I_h S_v}{(\sigma_v(t) N_v + \sigma_h N_h)^2}, \\
\frac{d\lambda_2}{dt} &= \lambda_2 \mu_h + (\lambda_2 - \lambda_3) \kappa_h + (\lambda_2 - \lambda_1) \frac{\sigma_v(t) \sigma_h^2 \beta_{vh} I_v S_h}{(\sigma_v(t) N_v + \sigma_h N_h)^2} + (\lambda_{10} - \lambda_9) \frac{\sigma_v(t) \sigma_h^2 \beta_{hv} I_h S_v}{(\sigma_v(t) N_v + \sigma_h N_h)^2}, \\
\frac{d\lambda_3}{dt} &= -C_1 + \lambda_3(\mu_h + d_h) + \alpha_h(\lambda_3 - \lambda_4) + (\lambda_2 - \lambda_1) \frac{\sigma_v(t) \sigma_h^2 \beta_{vh} I_v S_h}{(\sigma_v(t) N_v + \sigma_h N_h)^2} + (\lambda_9 - \lambda_{10}) \frac{\sigma_v(t) \sigma_h \beta_{hv} S_v}{\sigma_v(t) N_v + \sigma_h N_h} \\
&\quad + (\lambda_{10} - \lambda_9) \frac{\sigma_v(t) \sigma_h^2 \beta_{hv} I_h S_v}{(\sigma_v(t) N_v + \sigma_h N_h)^2}, \\
\frac{d\lambda_4}{dt} &= \lambda_4 \mu_h + (\lambda_4 - \lambda_1) \gamma_h + (\lambda_2 - \lambda_1) \frac{\sigma_v(t) \sigma_h^2 \beta_{vh} I_v S_h}{(\sigma_v(t) N_v + \sigma_h N_h)^2} + (\lambda_{10} - \lambda_9) \frac{\sigma_v(t) \sigma_h^2 \beta_{hv} I_h S_v}{(\sigma_v(t) N_v + \sigma_h N_h)^2}, \\
\frac{d\lambda_5}{dt} &= \lambda_5 \mu_a + (\lambda_5 - \lambda_6) \frac{\sigma_v(t) \sigma_a \beta_{va} I_v}{\sigma_v(t) N_v + \sigma_a N_a} + (\lambda_6 - \lambda_5) \frac{\sigma_v(t) \sigma_a^2 \beta_{va} I_v S_a}{(\sigma_v(t) N_v + \sigma_a N_a)^2} + (\lambda_{10} - \lambda_9) \frac{\sigma_v(t) \sigma_a^2 \beta_{av} I_a S_v}{(\sigma_v(t) N_v + \sigma_a N_a)^2}, \\
\frac{d\lambda_6}{dt} &= \lambda_6 \mu_a + (\lambda_6 - \lambda_7) \kappa_a + (\lambda_6 - \lambda_5) \frac{\sigma_v(t) \sigma_a^2 \beta_{va} I_v S_a}{(\sigma_v(t) N_v + \sigma_a N_a)^2} + (\lambda_{10} - \lambda_9) \frac{\sigma_v(t) \sigma_a^2 \beta_{av} I_a S_v}{(\sigma_v(t) N_v + \sigma_a N_a)^2}, \\
\frac{d\lambda_7}{dt} &= -C_2 + \lambda_7(\mu_a + d_a) + \alpha_a(\lambda_7 - \lambda_8) + (\lambda_6 - \lambda_5) \frac{\sigma_v(t) \sigma_a^2 \beta_{va} I_v S_a}{(\sigma_v(t) N_v + \sigma_a N_a)^2} + (\lambda_9 - \lambda_{10}) \frac{\sigma_v(t) \sigma_a \beta_{av} S_v}{\sigma_v(t) N_v + \sigma_a N_a} \\
&\quad + (\lambda_{10} - \lambda_9) \frac{\sigma_v(t) \sigma_a^2 \beta_{av} I_a S_v}{(\sigma_v(t) N_v + \sigma_a N_a)^2}, \\
\frac{d\lambda_8}{dt} &= \lambda_8 \mu_a + (\lambda_8 - \lambda_5) \gamma_a + (\lambda_6 - \lambda_5) \frac{\sigma_v(t) \sigma_a^2 \beta_{va} I_v S_a}{(\sigma_v(t) N_v + \sigma_a N_a)^2} + (\lambda_{10} - \lambda_9) \frac{\sigma_v(t) \sigma_a^2 \beta_{av} I_a S_v}{(\sigma_v(t) N_v + \sigma_a N_a)^2}, \\
\frac{d\lambda_9}{dt} &= \lambda_9(\mu_v(t) + u_2(t)) + (\lambda_2 - \lambda_1) \frac{\sigma_v^2(t) \sigma_h \beta_{vh} I_v S_h}{(\sigma_v(t) N_v + \sigma_h N_h)^2} + (\lambda_6 - \lambda_5) \frac{\sigma_v^2(t) \sigma_a \beta_{va} I_v S_a}{(\sigma_v(t) N_v + \sigma_a N_a)^2} \\
&\quad + (\lambda_9 - \lambda_{10}) \frac{\sigma_v(t) \sigma_h \beta_{hv} I_h}{\sigma_v(t) N_v + \sigma_h N_h} + (\lambda_9 - \lambda_{10}) \frac{\sigma_v(t) \sigma_a \beta_{av} I_a}{\sigma_v(t) N_v + \sigma_a N_a} \\
&\quad + (\lambda_{10} - \lambda_9) \frac{\sigma_v^2(t) \sigma_a \beta_{av} I_a S_v}{(\sigma_v N_v + \sigma_a N_a)^2} + (\lambda_{10} - \lambda_9) \frac{\sigma_v^2(t) \sigma_h \beta_{hv} I_h S_v}{(\sigma_v(t) N_v + \sigma_h N_h)^2},
\end{aligned}$$

$$\begin{aligned}
\frac{d\lambda_{10}}{dt} &= \lambda_{10}(\mu_v(t) + u_2(t)) + \kappa_v(t)(\lambda_{10} - \lambda_{11}) + (\lambda_2 - \lambda_1) \frac{\sigma_v^2(t)\sigma_h\beta_{vh}I_vS_h}{(\sigma_v(t)N_v + \sigma_hN_h)^2} + (\lambda_6 - \lambda_5) \frac{\sigma_v^2(t)\sigma_a\beta_{va}I_vS_a}{(\sigma_v(t)N_v + \sigma_aN_a)^2} \\
&\quad + (\lambda_{10} - \lambda_9) \frac{\sigma_v^2(t)\sigma_a\beta_{av}I_aS_v}{(\sigma_v(t)N_v + \sigma_aN_a)^2} + (\lambda_{10} - \lambda_9) \frac{\sigma_v^2(t)\sigma_h\beta_{hv}I_hS_v}{(\sigma_v(t)N_v + \sigma_hN_h)^2}, \\
\frac{d\lambda_{11}}{dt} &= \lambda_{11}(\mu_v(t) + u_2(t)) + (\lambda_1 - \lambda_2) \frac{\sigma_v(t)\sigma_h\beta_{vh}S_h}{\sigma_v(t)N_v + \sigma_hN_h} + (\lambda_2 - \lambda_1) \frac{\sigma_v^2(t)\sigma_h\beta_{vh}I_vS_h}{(\sigma_v(t)N_v + \sigma_hN_h)^2} \\
&\quad + (\lambda_5 - \lambda_6) \frac{\sigma_v(t)\sigma_a\beta_{va}S_a}{\sigma_v(t)N_v + \sigma_aN_a} + (\lambda_6 - \lambda_5) \frac{\sigma_v^2(t)\sigma_a\beta_{va}I_vS_a}{(\sigma_v(t)N_v + \sigma_aN_a)^2} + (\lambda_{10} - \lambda_9) \frac{\sigma_v^2(t)\sigma_a\beta_{av}I_aS_v}{(\sigma_v(t)N_v + \sigma_aN_a)^2} \\
&\quad + (\lambda_{10} - \lambda_9) \frac{\sigma_v^2(t)\sigma_h\beta_{hv}I_hS_v}{(\sigma_v(t)N_v + \sigma_hN_h)^2}. \tag{13}
\end{aligned}$$

In addition, the optimal solution of the Hamiltonian are determined by taking the partial derivatives of the function $H(t)$ in (12) with respect to control functions u_i , followed by setting the resultant equation to zero and then solve for u_i^* , $i = 1, 2$ follows:

$$\frac{\partial H}{\partial u_1} = u_1^* W_1 - (\lambda_1 - \lambda_4) S_h. \tag{14}$$

$$\frac{\partial H}{\partial u_2} = u_2^* W_2 - (\lambda_9 S_v + \lambda_{10} E_v + \lambda_{11} I_v). \tag{15}$$

Observe that $\frac{\partial^2 H}{\partial u_i^2} = W_i > 0$ and this demonstrates that the optimal control problem has minimum value at the optimal solution $U^*(t)$. Furthermore by setting (15) to zero and solve for u_i^* gives

$$u_1^* = \frac{(\lambda_1 - \lambda_4) S_h}{W_1}, \quad u_2^* = \frac{(S_v \lambda_9 + E_v \lambda_{10} + I_v \lambda_{11})}{W_2}.$$

By applying the the standard arguments and the bounds for the controls, we obtain the characterization of the optimal controls as follows:

$$u_i = \min \left\{ q_i, \max \left(0, u_i^* \right) \right\}. \tag{16}$$



AIMS Press

©2020 the Author(s), licensee AIMS Press. This is an open access article distributed under the terms of the Creative Commons Attribution License (<http://creativecommons.org/licenses/by/4.0>)